LA-UR-12-20244

Title: Modeling Aeolian Transport of Contaminated Sediments at Los Alamos National Laboratory, Technical Area 54, Area G: Sensitivities to Succession, Disturbance, and Future Climate

Author(s):   Whicker, Jeffrey J.
Kirchner, Thomas B.
Breshears, David D.
Field, Jason P.

Intended for: Report

Los Alamos
NATIONAL LABORATORY
——— EST.1943 ———

Modeling Aeolian Transport of Contaminated Sediments at Los Alamos National Laboratory, Technical Area 54, Area G: Sensitivities to Succession, Disturbance, and Future Climate

Authors:
Jeffrey J. Whicker[1]
Thomas B. Kirchner[2]
David D. Breshears[3]
Jason P. Field[4]

Date:
February 2012

Table of Contents_____

List of Figures _____

List of Tables _____

Acronyms and Abbreviations _____

BSNE	Big Springs Number Eight
DOE	U.S. Department of Energy
LANL	Los Alamos National Laboratory
MDA	Material Disposal Area
TA-54	Technical Area 54
TEOM	Tapered Element Oscillating Microbalance
VMTran	Vegetation Modified Transport (model)

1.0 Introduction

The Technical Area 54 (TA-54) Area G disposal facility is used for the disposal of radioactive waste at Los Alamos National Laboratory (LANL). U.S. Department of Energy (DOE) Order 435.1 (DOE, 2001) requires that radioactive waste be managed in a manner that protects public health and safety and the environment. In compliance with that requirement, DOE field sites must prepare and maintain site-specific radiological performance assessments for facilities that receive waste after September 26, 1988. Sites are also required to conduct composite analyses for facilities that receive waste after this date; these analyses account for the cumulative impacts of all waste that has been (and will be) disposed of at the facilities and other sources of radioactive material that may interact with these facilities.

LANL issued Revision 4 of the Area G performance assessment and composite analysis in 2008 (LANL, 2008). In support of those analyses, vertical and horizontal sediment flux data were collected at two analog sites, each with different dominant vegetation characteristics, and used to estimate rates of vertical resuspension and wind erosion for Area G (Whicker and Breshears, 2005). The results of that investigation indicated that there was no net loss of soil at the disposal site due to wind erosion, and suggested minimal impacts of wind on the long-term performance of the facility. However, that study did not evaluate the potential for contaminant transport caused by the horizontal movement of soil particles over long time frames. Since that time, additional field data have been collected to estimate wind threshold velocities for initiating sediment transport due to saltation and rates of sediment transport once those thresholds are reached. Data such as these have been used in the development of the Vegetation Modified Transport (VMTran) model. This model is designed to estimate patterns and long-term rates of contaminant redistribution caused by winds at the site, taking into account the impacts of plant succession and environmental disturbance.

Aeolian, or wind-driven, sediment transport drives soil erosion, affects biogeochemical cycles, and can lead to the transport of contaminants (Pye, 1987; Chadwick et al., 1999; Toy et al., 2002; Jickells et al., 2005; Whicker et al., 2006a; Field et al., 2010). Rates of aeolian sediment transport depend in large part on the type, amount, and spatial pattern of vegetation (Gillette and Passi, 1988; Stockton and Gillette, 1990; Gillette and Chen, 2001; Li et al., 2007; Okin, 2008; Breshears et al., 2009). In particular, the amount of cover from trees and shrubs, which act as roughness elements (Wolfe and Nickling, 1993), alters rates of aeolian sediment transport (Breshears et al., 2009). The degree to which the understory is disturbed (Lee, 1991; Breshears et al., 2009) and the associated spacing of bare soil gaps (Okin and Gillette, 2001; Okin, 2008) further influence sediment transport rates. Changes in vegetation structure and patterns over periods of years to centuries may have profound impacts on rates of wind-driven transport (Neilson, 1995; Swetnam and Betancourt, 1998; Breshears et al., 2009).

For recently disturbed areas, succession is likely to occur through a series of vegetation communities (Horn, 1974; Huston and Smith, 1987; Pickett et al., 1987; Glenn-Lewin and van der Maarel, 1992). Area G currently exhibits a mosaic of vegetation cover (Figure 1-1), with
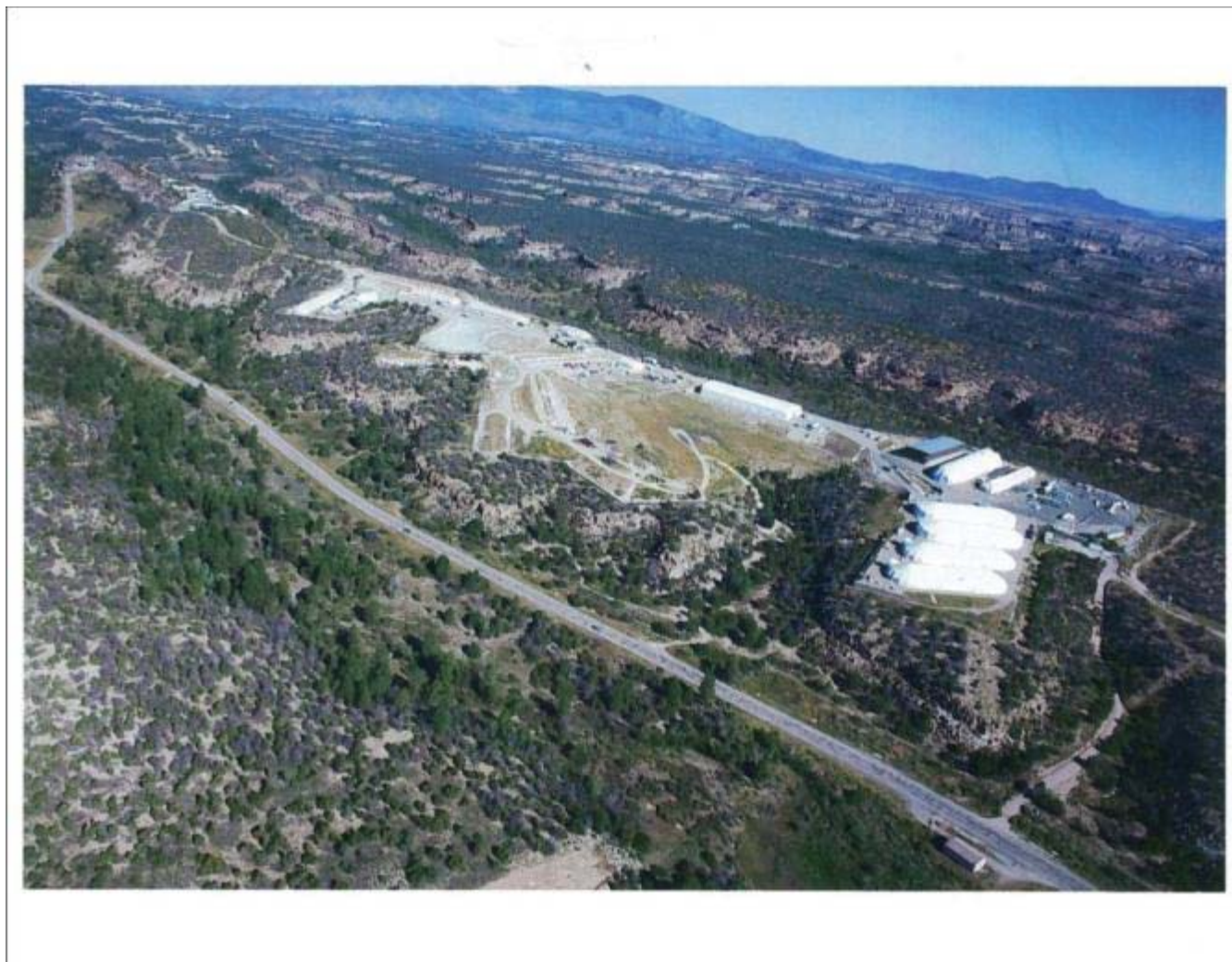
**Figure 1-1
Aerial View of Area G Showing Current Vegetation Patterns**

patches of grass and forbs over closed disposal units, and bare ground in heavily used portions of the site. These areas are surrounded by less disturbed regions of shrubland and piñon-juniper woodland; some ponderosa pine forest is also visible in the canyon along the road. The successional trajectory for the disturbed portions of Area G is expected to proceed from grasses and forbs (which would be established during site closure), to shrubs such as chamisa, to a climax community of piñon-juniper woodland (Figure 1-2). Although unlikely under current conditions, a ponderosa pine forest could develop over the site if the future climate is wetter.

In many ecosystems, substantial and often periodic disturbances such as fire or severe drought can rapidly alter vegetation patterns (Turner et al., 1998; Whicker et al., 2002; Allen, 2007; Romme et al., 2009). Such disturbances are likely to increase in the southwestern United States where projections call for a warmer and drier climate. (Breshears et al., 2005a; Westerling et al., 2006; Adams et al., 2009). With respect to Area G, the three most likely disturbance types are surface fire, crown fire, and drought-induced tree mortality. Each type of disturbance has a different frequency or likelihood of occurrence, but all three tend to reset the vegetation succession cycle to earlier stages (Figure 1-3).

The Area G performance assessment and composite analysis evaluate the impacts of disposing of radioactive waste over a period of hundreds to thousands of years. An assessment of aeolian sediment transport over this timeframe needs to account for the impacts of changes in vegetation structure and other surface conditions that occur under normal circumstances and as a result of environmental disturbance. Recent aeolian sediment transport studies undertaken in diverse dryland systems on both undisturbed and disturbed lands have yielded a suite of empirical measurements (Neff et al., 2008; Breshears et al., 2009; Bergametti and Gillette., 2010; Dong et al., 2010; Díaz-Nigenda et al., 2010; Flores-Aqueveque et al., 2010; Field et al., 2010). However, these studies do not take into account changes in long-term conditions at the sites being investigated. Although studies of dune systems have begun to account for different types of vegetation due to succession and the effects of disturbance under current and projected climate (Baas, 2002; Baas and Nield, 2007; Nield and Baas, 2008; Kim and Yu, 2009; Baas and Nield, 2010), similar information for drylands that are not dominated by dunes is almost entirely lacking.

Development of the VMTran model was undertaken as a means for evaluating the potential long-term impacts of horizontal sediment transport on the redistribution of contaminated soils at Area G. The model is tightly coupled to the suite of empirical dryland measurements discussed above and the field data collected during this investigation, and is capable of accounting for the effects of succession, disturbances due to fire and drought, and changes in climate.

This report describes an investigation conducted using the VMTran model to estimate the potential for, and impacts of, aeolian sediment transport at Area G over extended periods of time. The methods used to conduct the field investigations and the objectives of the VMTran model development effort are described in Section 2. The results of the investigation are presented and discussed in Sections 3 and 4, respectively.

Grassland

Shrubland

Woodland

**Figure 1-2
Anticipated Vegetation Succession at Area G after
Closure: Grassland to Shrubland to Woodland**

Early succession
landfill cover

Succession

Mature
piñon-juniper
woodland

Disturbance

Surface Fire

Crown Fire

Drought-Induced
Plant Die-off
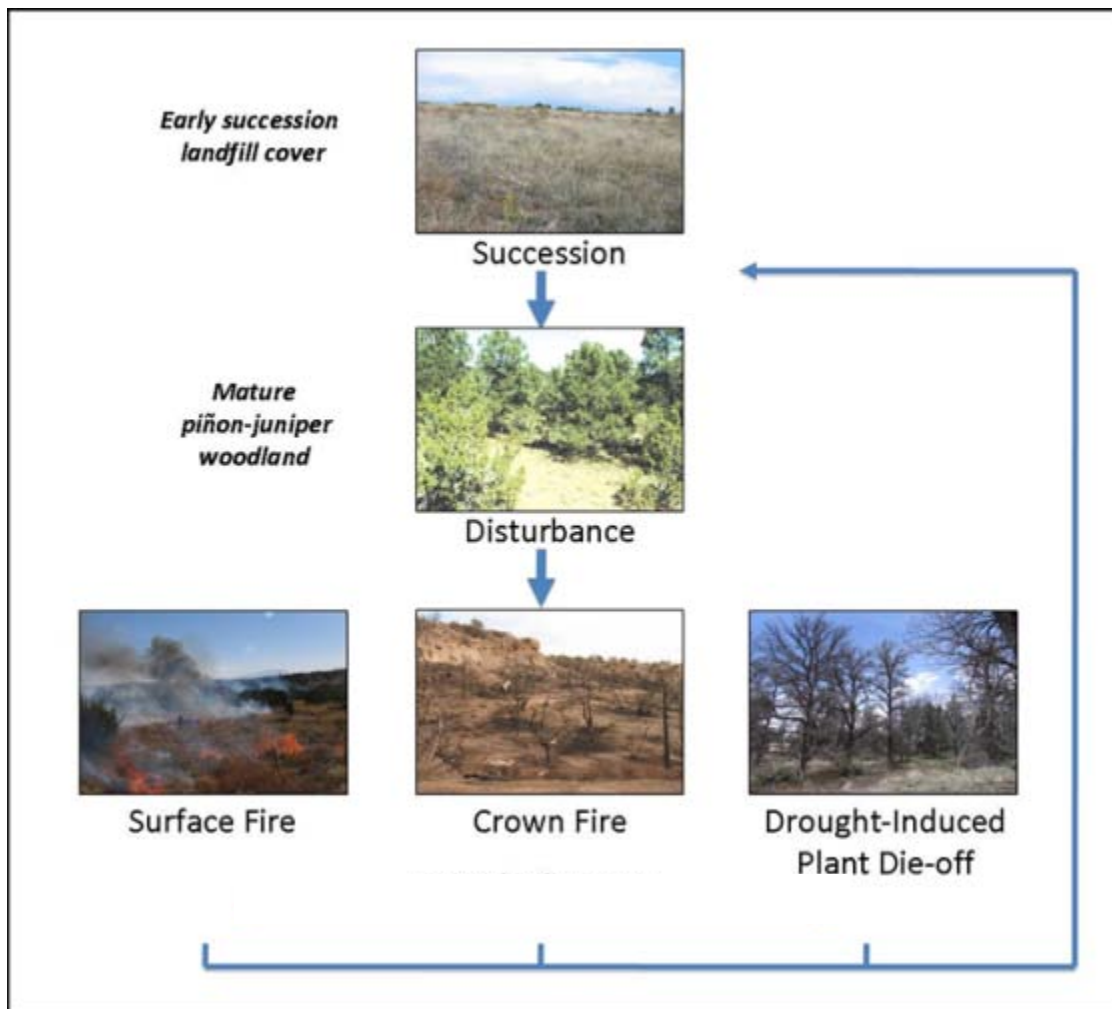
**Figure 1-3
Disturbances Cause the Vegetation Succession Cycle to Revert to Earlier Stages**

2.0 Methods

The investigation into the long-term impacts of aeolian sediment transport included the collection of field data needed to support the modeling and the development of the VMTran model. The methods used to conduct the field measurements are discussed in Section 2.1 and the model development effort is addressed in Section 2.2. Section 2.3 concludes with a description of the simulations that were conducted using VMTran.

2.1 Field Measurements

Field measurements were conducted at two analog sites located near Area G. The first site, MDA J, is characterized as grassland, which is the first successional stage expected to occur at Area G following closure. The second site, located at TA-51, is a piñon-juniper woodland and is representative of the climax condition expected at Area G. Following characterization of these sites, a series of measurements was collected using the methods described below.

2.1.1 Site Characterization

Cover conditions were characterized at each analog site using standardized techniques that have been used to monitor grasslands, shrublands, and savanna ecosystems (Herrick et al., 2005). Three 30.5-m (100-ft) transects were established, extending outward from the center of each sampling area. Cover characteristics were determined at 0.61-m (2-ft) intervals along each transect. The ground/vegetation cover at each point was categorized by type (e.g., soil, forb, grass, rock, litter, biological soil crust, tree, duff, and dead branch). Data for each point along the three transects were combined to estimate totals for the grassland and woodland sites that could be characterized as (1) bare soil, (2) basal cover (lower-level cover such as grasses, litter, rocks, and forbs), and (3) tree canopy cover. A second set of measurements used the same radial transects to measure the distance between gaps in vegetation cover (along the ground) and gaps in the tree canopy at the woodland site.

2.1.2 Wind Threshold Velocity Measurements

As it applies here, the threshold velocity is defined as the wind velocity required to move, or entrain, particles of soil or sediment. Measurements of threshold velocity were taken with the intent of using them to estimate the number of annual wind-erosion events for the VMTran modeling. Originally, these measurements were conducted using a Sensit instrument to determine saltation activity as a function of micro-meteorological conditions at the study sites. The Sensit instrument has a piezoelectric crystal that detects the impacts of saltating soil particles in real time; correlating the particle impacts with simultaneously measured wind velocities provides a means for estimating threshold wind velocities. A Sensit instrument was placed at each study site and data were collected from April 2009 until July 2010. Analysis of the

Sensit data from the two sites showed that the only significant detections made by the instrument were from raindrop splash. Consequently, it was not possible to establish wind erosion threshold velocities using the Sensit data.

A Tapered Element Oscillating Microbalance (TEOM), located at TA-6, proved to be a more sensitive instrument for detecting increases in aerosol as a function of wind speed. Aerosol concentration data collected using the TEOM were combined with wind velocity data to determine threshold velocities indirectly. The TEOM was used to sample concentrations of particulates having a diameter of 10 μm or less that were suspended as a result of saltation (Zobeck et al. 2003). These measurements were compared to results from other studies to provide perspective on their applicability to the MDA J and TA-51 analog sites.

As the VMTran model developed, it became apparent that horizontal mass flux data collected over periods of time ranging from weeks to months were preferable to those collected during individual wind events. Using the long-term data to estimate annual averages yielded the most accurate estimates for the modeling; this conclusion is based on the assumption that wind conditions are, on average, relatively constant or that any changes would not be enough to significantly alter horizontal mass fluxes. Ultimately, then, the threshold velocity data were used only to help establish the fraction of time that high-wind events blew in different compass directions.

2.1.3 Horizontal Flux Measurements

Measurements of horizontal sediment flux were made using Big Springs Number Eight (BSNE) samplers (Fryrear, 1986); measurements were conducted from October 8, 2009 to July 15, 2010. The samplers have been used in prior studies at LANL, including the 2005 effort conducted in support of the Area G performance assessment and composite analysis (Whicker and Breshears, 2005; Whicker et al. 2006a,b). The measurements supported the identification of flux data needed for the VMTran modeling; the data collected in this study supplement data collected earlier and more fully address the high-wind periods that generally occur in the spring months. Figure 2-1 shows a BSNE sampling station at a LANL site that was previously burned. Similar arrangements of BSNE samplers were used in this study; four sampling stations, each with three BSNE samplers at heights of 0.25, 0.5, and 1 m (0.8, 1.6, and 3.3 ft) above the ground, were placed at the grassland and woodland analog sites. The horizontal fluxes were calculated as follows:

$$HMF = \frac{M}{A \times T}$$
<div align="right">1</div>

Where

HMF =   horizontal mass flux (g/m^2/yr)
M =   mass of sediment collected in sampler (g, dry weight)

Figure 2-1
A BSNE Sampling Station with Horizontal Mass Flux Samplers at Three Heights

A =   area of sampling port (1×10^{-3} m^2)

T =   time of collection (yr)

The sediment mass is an average of the quantities collected at the three sampling heights.

2.1.4   Aerosol Characterization

A Climet particle counter (model CI-500) was used to measure particle concentrations intermittently from June 26 through July 23, 2009. The particle counter was placed in a weatherproof housing on the edge of Area J; aerosol concentrations were collected over 1-hour intervals and classified by particle diameter.[1] Sampling was conducted during periods when wind speeds were relatively light (averaging less than 2 m/s [6.6 ft/s]). The housing was found to lower collection efficiencies for particles in the 5 to 10 μm (2.0×10^{-4} to 3.9×10^{-4} in.) and increase those for particles having diameters of tens of micrometers at wind velocities of 12 m/s (39 ft/s) (Rodgers et al., 2000); collection of data at lower wind speeds limits the impacts of this behavior. These measurements were conducted to qualitatively assess particle size distributions, most notably to distinguish between the regional dust load (particles less than 5 µm [2.0×10^{-4} in.] in diameter) and locally derived particles.

2.2   Model Development and Simulations

The VMTran model was developed to provide a means for estimating the impacts of aeolian sediment transport on contaminant redistribution over extended periods of time. The conceptual and mathematical models upon which VMTran is based are presented in Section 2.2.1. Several simulations were conducted to demonstrate the capabilities of the model; these model runs are described in Section 2.2.2.

2.2.1   Conceptual Model

The VMTran model simulates the vegetation-moderated, wind-driven transport of sediment. The effects of vegetation on sediment transport are two-fold: it is an important factor in determining the proportion of the soil surface that is exposed to suspension and it influences wind speeds at the surface. VMTran is notable in its ability to account for the effects of vegetation on rates and patterns of sediment transport and to simulate the impacts of changes in the plant community that accompany disturbance and succession. The disturbances modeled include surface fire, crown fire, and drought. Succession modeling accounts for passage of the site from a grassland-dominated community to woodland or forest; the possible impacts of climate change on the trajectory of plant succession may also be taken into consideration.

---

[1] Particle diameters were placed into the following bins: < 0.3, 0.3–0.5, 0.5–1.0, 1.0–5.0, 5.0–10 and 10–25 µm ($<1.2 \times 10^{-5}$, 1.2×10^{-5}–2.0×10^{-5}, 2.0×10^{-5}–3.9×10^{-5}, 3.9×10^{-5}–2.0×10^{-4}, 2.0×10^{-4}–3.9×10^{-4}, and 3.9×10^{-4}–9.8×10^{-4} in.)

2.2.2 Mathematical Model

The site under consideration is discretized at a number of levels so it can be modeled using VMTran (Figure 2-2). Contamination on the soil surface is represented using a series of evenly spaced points; each point is assigned a contaminant concentration. Mapped on top of these points, and centered on the area of interest, are overlapping grids, each composed of n by n cells (four grids with five cells to a side are shown in Figure 2-2). Each grid is oriented such that each side is perpendicular to a specific wind direction. Multiple grids are required to simulate the transport of sediment in more than four directions; the four grids shown in the figure are used to account for the 16 wind directions seen in a typical wind rose. The number of cells used to construct each grid may be specified by the model user, but the cell dimensions are held constant at 50×50 m (164×164 ft).

2.2.2.1 Succession Modeling

VMTran simulates ecological succession by dividing the surface of each 50×50 m (164×164 ft) cell into 1-m^2 (10.8-ft^2) quadrats and using a Markov-like transition matrix to simulate changes in conditions within each quadrat. Each quadrat is assigned a cover type such as trees (piñon, juniper, or ponderosa pine), shrubs, grasses (including forbs), litter, or bare soil. The transition matrix specifies the annual probability that the cover type in a given quadrat will change to another cover type or remain the same. To illustrate, the transition matrix for intercanopy areas is provided in the upper portion of Table 2-1; the probabilities listed in this table are included in VMTran as default values. As shown in the table, the probability that bare soil in the intercanopy areas will become grass-covered over the course of a year is 0.05; the quadrat is expected to persist as bare soil 95 percent of the time. Once grass has become established, the quadrat may remain grass-covered (93 percent of the time) or transition to bare soil or shrubs. Shrubs are expected to persist 74 percent of the time, but transitions to trees or bare soil may also occur.

The canopies of trees and shrubs can grow beyond the bounds of the cover cell where they are rooted. Because the impact of shading on understory plants is significant, the model employs one transition matrix for intercanopy quadrats and another for under-canopy quadrats; the under-canopy quadrat is included as the second half of Table 2-1. In the default under-canopy matrix, a bare soil quadrat can transition only to a grass or litter quadrat, and grass quadrats can transition only to bare soil or litter (Table 2-1). A quadrat categorized as litter will remain litter unless the woody plants above it are removed, at which point it becomes an intercanopy quadrat. Thus, litter will rapidly dominate the under-canopy quadrats. Because some woody plants can over-top other woody plants, the transition matrix includes transitions to other types of cover cells (e.g., trees can die and the cover cell revert to bare soil).
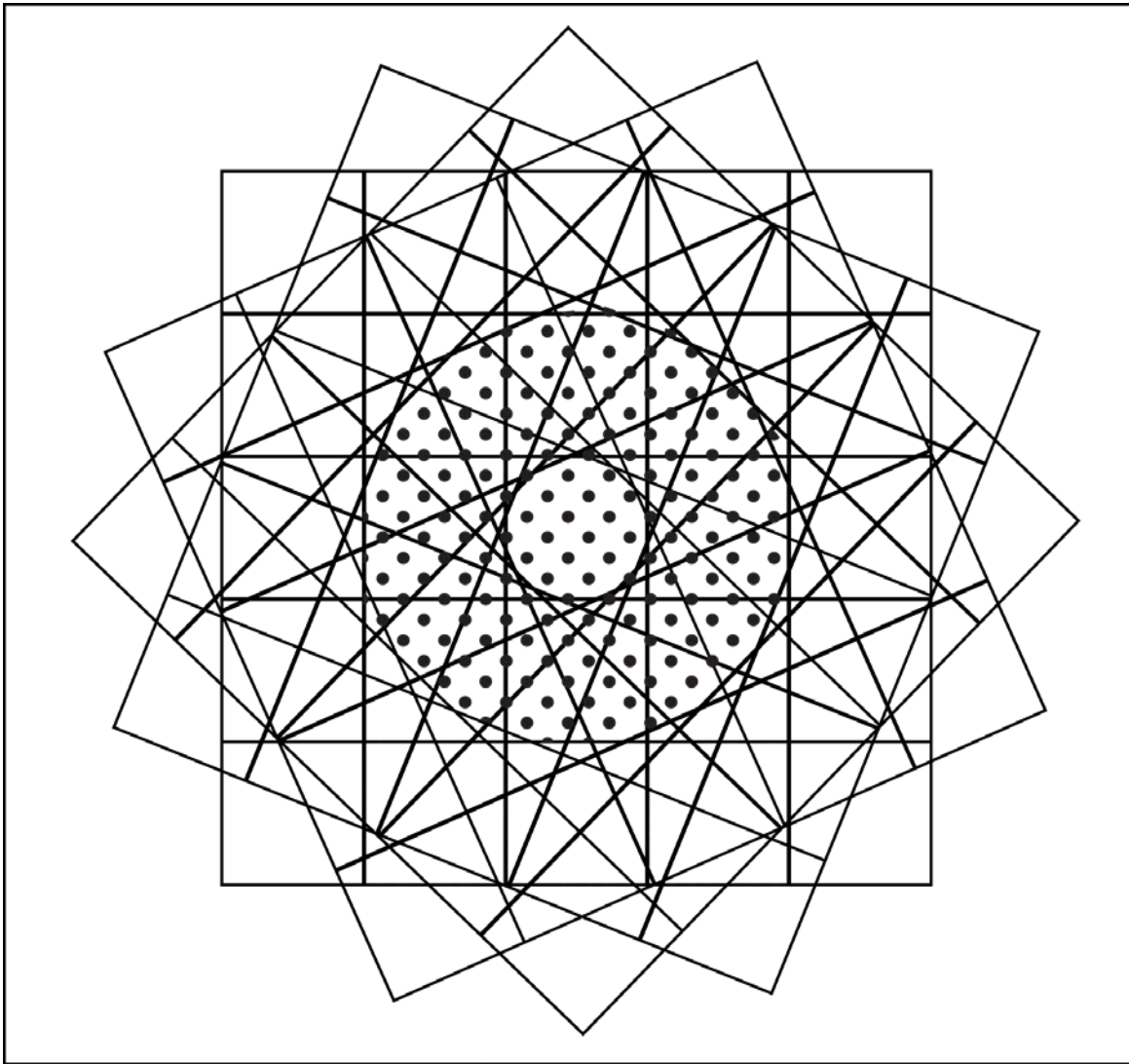
Figure 2-2
Discretized Domain Used in the VMTran Model

Table 2-1
Cover Transition Matrix for Intercanopy Areas and under Tree Canopies

To	From: Soil	Litter	Grass	Shrubs	Piñon	Juniper	Ponderosa
Intercanopy Areas							
Soil	0.95	0.08	0.01	0.01	0.023	0.023	0.02
Litter	0	0.92	0	0	0	0	0
Grass	0.05	0	0.93	0	0	0	0
Shrubs	0	0	0.06	0.74	0	0	0
Piñon	0	0	0	0.125	0.977	0	0
Juniper	0	0	0	0.125	0	0.977	0
Ponderosa	0	0	0	0	0	0	0.98
Under-canopy Areas							
Soil	0.89	0	0.01	0.04	0.023	0.023	0.02
Litter	0.06	1	0.06	0	0	0	0
Grass	0.05	0	0.93	0	0	0	0
Shrubs	0	0	0	0.71	0	0	0
Piñon	0	0	0	0.125	0.977	0	0
Juniper	0	0	0	0.125	0	0.977	0
Ponderosa	0	0	0	0	0	0	0.98

The transition matrices shown in Table 2-1 are "Markov-like" because, for computational efficiency, the age of the plants in the cover cells is tracked and used to delay the onset of the growth of woody plants. For example, cover cells containing shrubs cannot transition to trees until they reach a specified age. In a traditional Markov approach, age dependencies would be handled by having cover cells of the same type (e.g., shrub), but with ages attached. Hence a shrub of age 1 could either die, be replaced by another growth form, or transition to a shrub of age 2. In this model, aging is represented by incrementing an age counter for the quadrat.

The transition in a quadrat's state is a stochastic process and generally independent of transitions in other quadrats. An exception occurs, however, for quadrats in which trees and shrubs exist because these plants can extend their influence on neighboring cells through the effects of shading. VMTran simulates the growth of the canopy of a woody plant by assuming that growth is logistic when not shaded by taller woody plants. When the canopies of neighboring woody

plants overlie one another, it is assumed that the growth rate of the smaller plant is reduced proportional to the area of its canopy that lies beneath the canopy of the taller plant. Thus,

$$\frac{dr_i}{dt} = g_i \left(1 - \frac{r_i}{R_i}\right)\left(1 - \frac{\sum_{j=1}^{n} A_{i,j}}{\pi r_i^2}\right)$$

2

and

$$A_{i,j} = r_i^2 \cos^{-1}\left(\frac{d_{i,j}^2 + r_i^2 - r_j^2}{2 d r_i}\right) + r_j^2 \cos^{-1}\left(\frac{d_{i,j}^2 + r_j^2 - r_i^2}{2 d_{i,j} r_j}\right)$$
$$- \frac{1}{2}\sqrt{\left(-d_{i,j} + r_i + r_j\right)\left(d_{i,j} + r_i - r_j\right)\left(d_{i,j} - r_i + r_j\right)\left(d_{i,j} + r_i + r_j\right)} \; ; \; r_j \geq r_i$$

3

Where

dr_i/dt = differential rate of change in radius of plant i with time
r_i = the radius of the canopy of plant i
R_i = the maximum radius of the plant canopy of plant i
g_i = the intrinsic growth rate of plant i
$A_{i,j}$ = the area between the canopies of the ith and j[th] plants
r_j = the radius of the canopy of plant j??
$d_{i,j}$ = the distance between the ith and j[th] plants

Neighboring plants are those whose quadrats occur within the radius $\bar{R} = R_i + R_{max}$, where R_{max} is the maximum radius across all species. The intrinsic growth rate and maximum radius of a plant is defined for shrubs and each species of tree.

The objective of the succession modeling is to provide a time series of vegetative cover that can be used to estimate rates of aeolian sediment transport. The goal in parameterizing the succession model is to generate a realistic time series of plant density and canopy size distribution for trees and shrubs, similar to that observed under natural conditions. The transition matrices adopted for the modeling define the lifetimes of the plants and, therefore, plant density; the growth parameters selected for use will influence the size distribution.

Wangler and Minnich (1996) observed that shrubs increased in cover and density for 30 to 50 years following high-intensity fires in piñon-juniper woodlands of the San Bernardino Mountains, with *Pinus monophylla* becoming established 25 to 40 years after the fire. Mature shrubs acted as nurse plants, aiding in the establishment of piñon. Although the species of piñon that occurs at LANL differs from that studied by the Wangler and Minnich, the same general pattern of growth and replacement was assumed to occur in the forests of northern New Mexico. These observations support the assumption in the model that piñon will start replacing shrubs that have achieved an age of about 20 years. The transition probabilities from bare soil to grass and from grass to shrubs were set to achieve maximum shrub coverage in about 20 years. Although this is less time than was observed by Wangler and Minnich (1996), it is adopted to more closely mimic long-term shrub-cell densities. Cover cells can be assigned to only one type of vegetation. In the model, then, the number of shrub cells will decline after year 20 as shrub cells are reassigned to piñon. In reality, however, shrubs and piñons may coexist in the same cover cells for years after piñon is first established. Accelerating the peak for shrub growth in the model more closely approximates the shrub densities observed once the transition to trees has begun.

Martens et al. (1997) reported that *P. edulis* and *Juneriperus monosperma* occurred at densities of 314 and 350 trees per hectare, respectively, in a New Mexico forest. The transition probabilities from shrubs to piñon pine and from shrubs to juniper were adjusted to achieve these levels after approximately 150 years. Martens et al. (1997) also described the size distribution of *P. edulis* in a mature forest. The growth rate and transition probabilities used in VMTran were adjusted to produce a distribution that is similar to that presented in Martens et al. (1997); this distribution was achieved about 150 years after the start of succession.

Rates of sediment transport at Area G are a function of the successional stage of the disposal site and the amount of vegetative cover that is present. The successional stage is categorized in terms of the amount of woody plant canopy cover that is present (grassland has <10% woody plant canopy cover, shrubland has 10% to <30% woody canopy cover; woodland has 30% to <50% woody canopy cover; and forest has 50% or more woody plant canopy cover). Grassland, shrubland, and intercanopy areas within woodland and forest that have less than 10 to 60 percent bare ground are considered to be in an undisturbed state; a surface with 60 to 90 percent bare ground is considered to be disturbed.

The succession trajectory will be influenced by disturbances to the site and climatic changes. The VMTran model simulates three kinds of disturbances: surface fire, crown fire, and drought. The changes invoked by these events depend upon the type of disturbance, the successional stage present at the time of disturbance, and the degree of ground cover. Table 2-2 shows the successional transitions caused by the different types of disturbance. Although some disturbances cause a change in successional stage, others do not. For example, both surface fire and drought

are assumed to cause disturbed grassland to revert to bare soil. In contrast, woodland reverts to an earlier successional stage only in the event of a crown fire.

Table 2-2
Successional Stage and Ground Cover Conditions Following Disturbance

Successional Stage and Cover Condition Prior to Disturbance	Successional Stage and Cover Condition Following Disturbance		
	Surface Fire	Crown Fire	Drought
Grassland – disturbed	Bare	---[a]	Bare
Grassland –undisturbed	Grassland – disturbed	---[a]	Grassland – disturbed
Shrubland – disturbed	Shrubland – disturbed[b]	---[a]	Shrubland – disturbed[b]
Shrubland – undisturbed	Shrubland – disturbed	---[a]	Shrubland – disturbed
Woodland – disturbed	Woodland – disturbed	Shrubland – disturbed	Woodland or earlier – disturbed [c]
Woodland – undisturbed	Woodland – disturbed	Grassland – disturbed	Woodland or earlier – disturbed [c]
Forest – disturbed	Woodland – disturbed	Grassland – disturbed.	Woodland or earlier – disturbed[c]
Forest – undisturbed	Forest – disturbed	Woodland – disturbed	Forest or earlier – disturbed [c]

[a] *Crown fires do not affect grassland and shrubland communities.*

[b] *The shrubland disturbed state is maintained because the amount of woody cover is expected to be 10 percent or more or because maintaining the state as disturbed shrubland provides the highest (most conservative) sediment transport rates.*

[c] *Depending upon the tree species, drought may or may not cause woodland to revert to an earlier successional stage. For example, the more drought-tolerant junipers may persist but piñon pines may die.*

Post-disturbance reversions to an earlier successional stage are simulated by removing plants at random until the woody plant canopy cover target value is achieved. For example, to model the effects of a crown fire on undisturbed woodland, trees are removed until the canopy cover is less than 10 percent, at which point the successional stage is assumed to be grassland. The target values for other successional stages are selected at random from the range of values that defines the desired stage. The effects of drought are modeled in a similar fashion; woody plants are removed until the canopy cover value is achieved. However, whereas the effects of fire are assumed to be the same regardless of the woody plant species, the varying drought resistance of different trees is taken into account when modeling drought conditions (e.g., juniper is typically more drought resistant than piñon).

Grasses and forbs are removed in a similar fashion to reflect changes in ground cover that accompany disturbances. Quadrats within intercanopy areas are selected at random and plants
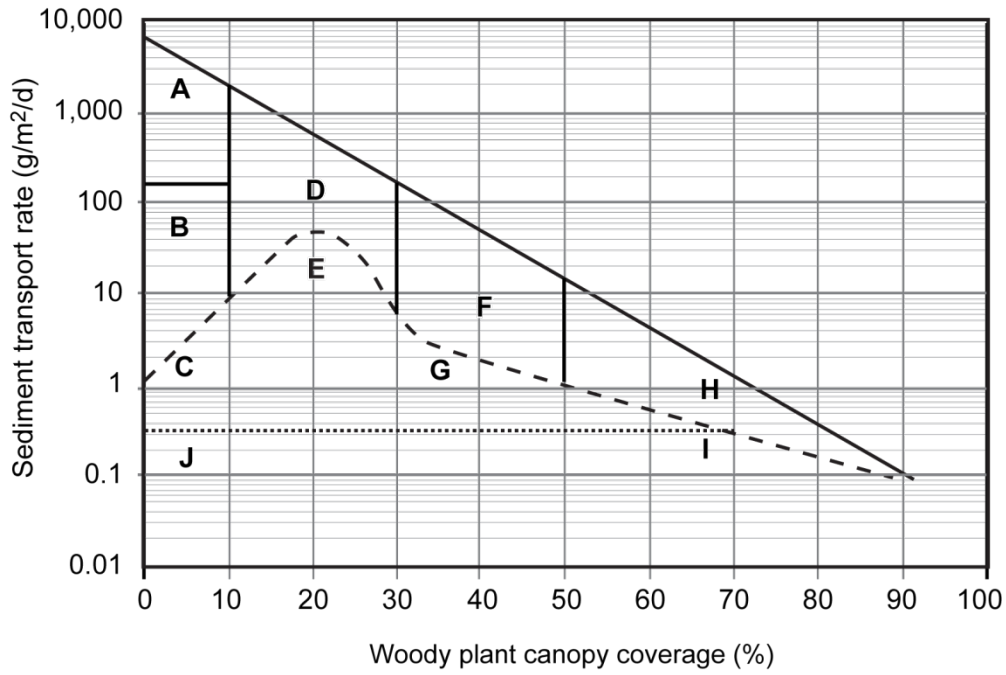
are removed until the fraction of the surface that is bare ground reaches the target value. The target value is selected randomly from the range of 60 to 90 percent when reverting to disturbed grassland and from 90 to 100 percent when bare ground is the final state.

The impacts of climate change on ecological succession are modeled by altering disturbance frequencies and by modifying the transition matrices. For example, transitions to ponderosa pine may be necessary to simulate the impacts of wetter conditions. A shift toward a drier climate may call for the total elimination of transitions to trees.

2.2.2.2 Sediment Transport Modeling

The sediment transport modeling operates at the scale of the 50×50-m (164×164-ft) cells; the flux of contaminated soil is computed on an annual basis and moved from one cell to the cell immediately downwind. The amount of contamination contained within each cell is the average of the values at each of the sampling points contained within the cell; sampling points may be contained by multiple, overlapping cells. Inspection of Figure 2-2 reveals that the intersection of the overlapping grids forms a mosaic of polygons. These polygons are irregular in size and shape and unsuitable for representing the soil surface in a computationally efficient way. Therefore, instead of tiling the surface with polygons and modeling the flow to and from each polygon, the surface is conceptualized as being defined by a regularly spaced mesh of points, where each point is envisioned as a sampling location of some fixed size (e.g., 1 m^2 [10.8 ft^2]) that is assumed to be representative of the surrounding area. The decision to conduct the transport modeling at the scale of the 50×50-m (164×164-ft) cells was dictated, to a large extent, by the nature of the empirical soil flux data collected in numerous field studies; the 50-m (164-ft) cell length is generally consistent with the distances traveled by saltating particles in vegetated areas (Shinn and Gouvieia, 1992; Baldocchi, 1997).

Rates of erosion are a function of the successional stage and the surface cover conditions. Figure 2-3 summarizes the sediment transport rates that are used to model the disturbed and undisturbed successional stages; these rates correspond to the multi-month transport estimates developed by Breshears et al. (2009) for a grassland-forest continuum. Extreme rates of sediment transport occur when the total vegetative cover is less than 10 percent and no woody vegetation is present (category A in Figure 2-3) and when more than 90 percent of the quadrats are vegetated (category J). The sediment transport rates adopted for the modeling are also summarized in Table 2-3.

Category	Description	Nominal sediment transport rate (g/m²/d)
A	Bare - no woody canopy cover	2000
B	Grassland - moderately disturbed	60
C	Grassland - undisturbed	2
D	Shrubland - disturbed	120
E	Shrubland - undisturbed	20
F	Woodland - disturbed	8
G	Woodland - undisturbed	1.4
H	Forest - disturbed	1.2
I	Forest - undisturbed	0.4
J	High ground cover	0.2

Figure 2-3
Sediment Transport Rates for Various Successional Stages (Breshears et al., 2009)

Table 2-3
Sediment Transport Rates for Successional Stages by Cover
Condition and Percentage of Bare Soil

	Sediment Transport Rate (g/m²/d)			
	Undisturbed Cover Condition		Disturbed Cover Condition	
Successional Stage	Bare Soil < 10%	Bare Soil 10 to < 60%	Bare Soil 60 to < 90%	Bare Soil 90 to 100%
Grassland	0.2	2	60	2,000
Shrubland	0.2	20	120	2,000
Piñon-Juniper Woodland	0.2	1.4	8	2,000
Ponderosa Pine Forest	0.2	0.4	1.2	2,000

Sediment within a given cell is transported when winds exceed the threshold velocity for suspension. The quantities of sediment and any associated contamination that are carried downwind are a function of the horizontal mass flux, which is itself a function of the condition and type of vegetative cover. For modeling purposes, the horizontal mass flux is set equal to the average annual sediment transport rates shown in Figure 2-3 and Table 2-3. The erosion mass flux for the cell is calculated by averaging the quadrat-specific sediment fluxes over the 50 × 50-m (164 × 164-ft) area.

The horizontal mass flux is used to calculate the rate of surface soil loss and the fractional rate of loss within the cell as follows:

$$SSL = \frac{HMF}{\rho_{soil}}$$

4

Where

SSL = surface soil loss rate (m/yr)
HMF = horizontal mass flux (g/m²/yr)
ρ_{soil} = density of soil (g/m³)

and

$$FLR = \frac{SSL}{D}$$

5

Where

FLR = fractional soil mass loss (per year)

D = depth (m)

The fractional loss rate is set equal to zero if the product of the surface soil loss rate and the simulation time is greater than the thickness of the sediment layer being modeled.

The model distributes the lost material by wind direction, taking into account the number of wind erosion events per year. Normalized directional wind frequencies were estimated using wind rose data for winds having velocities equal to or greater than a threshold velocity of 5 m/s; these frequencies are provided in Table 2-4. All suspended sediment is assumed to be deposited in the first cell that it encounters downwind of the source cell.

Table 2-4
Distribution of Threshold Velocity Winds

Direction	% of Time that Wind Velocity Exceeds 5 m/s[a]	Direction	% of Time that Wind Velocity Exceeds 5 m/s[a]
N	6.30	S	11.83
NNE	6.64	SSW	13.40
NE	3.72	SW	12.95
ENE	1.92	WSW	10.59
E	1.47	W	7.76
ESE	1.24	WNW	8.90
SE	1.35	NW	4.84
SSE	2.82	NNW	4.27

[a] Percentages are normalized to 100 percent and are used to distribute the contamination in the downwind direction.

The VMTran model was developed to simulate the transport of sediment by saltation across the disposal site over extended periods of time and under changing vegetative conditions. The model also tracks the movement of radioactive contamination that accompanies the migration of sediments. For the Area G performance assessment and composite analysis, however, the transport of radionuclides is addressed by other models and, as a result, is not discussed here.

2.3 Model Simulations

The impacts of vegetation succession and disturbance on sediment transport at Area G over a 1,000 year simulation period were investigated using a series of VMTran model simulations. The effects of succession alone were considered in some of these simulations; no disturbances were assumed to occur over the simulation period. Other simulations considered the cumulative effects of succession and disturbance. The frequencies of disturbance were set to 30, 250, and 50 years for surface fire, crown fire, and drought-induced tree die-off, respectively. The disturbance frequencies were

doubled for the final simulations to consider the effects of increased disturbance brought about by changes in climate (Turner et al., 1998; Allen, 2007; Romme et al., 2009).

The VMTran simulations were conducted to demonstrate the capabilities of the computer code and to gain insight into the potential for contaminant redistribution at Area G. The meteorological parameters used in the modeling were based on annualized measurements collected from the TA-54 meteorological station just east of Area G. The sediment transport rates applied in the simulations were based on measured fluxes from Area J (grassland site) and Mesita del Buey (woodland site), supplemented by additional measurements (Figure 2-3). Vegetation succession parameters and disturbance frequencies matched those anticipated for the site after Area G undergoes final closure.

For modeling purposes, it was assumed that an area of $31,400 \text{ m}^2$ ($338,000 \text{ ft}^2$) was contaminated. This area, represented using a circle with a diameter of 200 m (65 ft), was assumed to be uniformly contaminated to a depth of 1 m (3.3 ft). Cells within the circle are referred to as on-site or interior cells, while the cells outside of this area are referred to as off-site or sink cells. The results of the simulations were normalized in terms of the percent of original contamination removed or deposited from the on-site and off-site cells, respectively. The normalized concentrations were averaged over the entire site and plotted through time.

3.0   Results

The results of the field study and the VMTran model simulations are presented below. Section 3.1 summarizes the field measurements; the result of the VMTran model simulations are presented and discussed in Section 3.2.

3.1   Field Measurements

The field effort characterized the grassland and woodland analog sites in terms of successional stage and conducted a series of measurements designed to understand erosion potential. The results of these efforts are presented in the following sections.

3.1.1   Site Characterization

The characterization data for the grassland and woodland sites are summarized in Figure 3-1. Clear differences are evident between the sites in terms of canopy cover, bare ground, and basal cover (e.g., grasses, forbs, litter, and rocks) (Figure 3-1a) The woodland site exhibited a 38 percent canopy cover; intercanopy areas were characterized by 44 percent basal cover, and 18 percent bare soil. No canopy cover occurred at the grassland site. Basal cover was encountered over 64 percent of the site; the remaining 36 percent of the site was bare ground. Using the classification scheme discussed earlier, the two sites qualify as undisturbed grassland and woodland.

Figure 3-1(b) shows the distribution of gap lengths of bare soil along the transects at the grassland and woodland sites, while Figure 3-1(c) shows the gap lengths between canopy cover at the woodland site. The proportion of bare soil patches at the grassland site was about twice that of the woodland site; the gap lengths of the bare soil patches at both sites were generally less than 100 cm (39.4 in). In terms of the gap lengths between canopy cover, intervals greater than 7.5 m (24.6 ft) were most common (Figure 3-1c).

3.1.2   Wind Threshold Velocities

Measurements conducted using the Sensit instrument indicated that very little saltation occurred during the 15-month measurement period. Overall, there were 19 registered impacts out of 15,000 measurement intervals; all but one of these impacts occurred on days with measurable rain (>0.025 cm [0.01 in.]) and were likely caused by rainsplash. The registered impact that occurred on the day without rain was associated with a maximum wind velocity of 10.9 m/s (35.6 ft/s); many other days had similar wind gusts, but no registered impacts. These results suggest that either the vegetation in the area was sufficient to prevent most saltation or that the Sensit instrument was not particularly sensitive to measuring saltation for the soil types on the mesa.
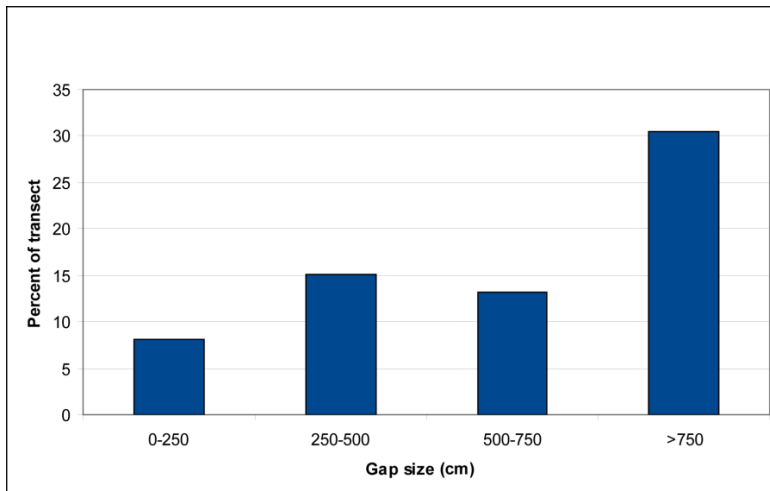
a. Percent canopy, bare ground, and basal cover
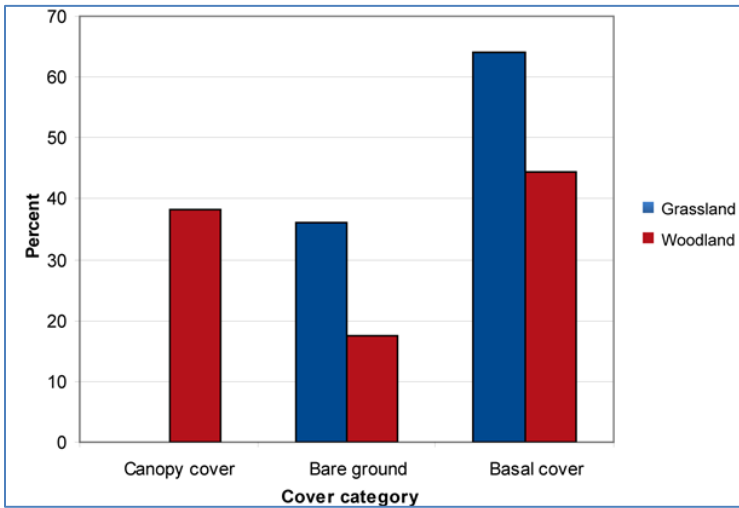
b. Distribution gap lengths for bare soil
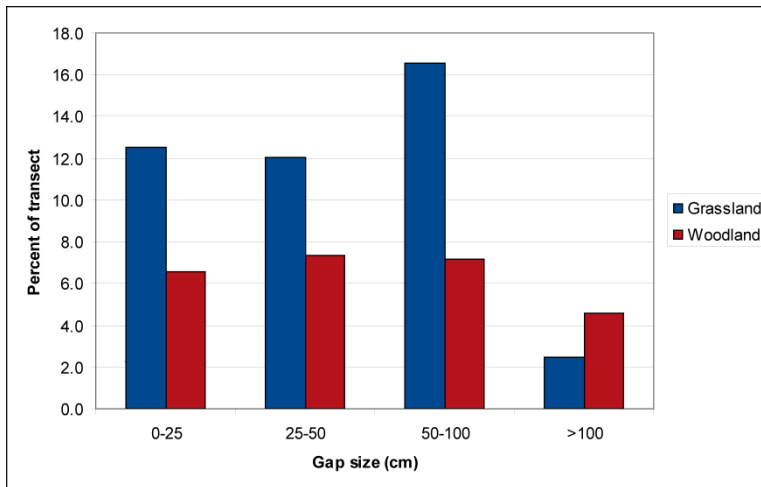
c. Distribution gap lengths for tree canopies

Figure 3-1
Cover Characteristics at the Grassland and Woodland Analog Sites

Measurements collected using a TEOM in an open area at TA-6 proved more useful than the Sensit data; the results of the TEOM sampling, shown in Figure 3-2, suggest a wind threshold velocity between 6 and 8 m/s (19.7 and 26.3 ft/s). These measurements are consistent with those collected in other studies. For example, Whicker et al. 2002 estimated threshold velocities of about 7 m/s (23 ft/s) at sites characterized by shrubs. The data collected using the TEOM were used to identify a threshold velocity that is consistent with the resolution of the Area G wind frequency and direction data. Those data are provided for a series of wind speed intervals; the interval that correlates best with the threshold velocities shown in Figure 3-2 ranges from 5 to 7.5 m/s (16.4 to 24.6 ft/s). Data for this interval and higher wind speed intervals were used to estimate the fraction of the time winds in excess of the threshold velocity blew in each direction (Table 2-4). This approach effectively defines the threshold velocity used in the modeling as 5 m/s (16.4 ft/s).

3.1.3   Horizontal Fluxes

The horizontal mass fluxes measured at the grassland and woodland sites are summarized in Figure 3-3. The mean fluxes measured at the grassland site are higher than those observed at the woodland site at all three sampling heights. The average fluxes measured at the two sites are compared to the sediment transport rates estimated by Breshears et al. (2009) for the different successional stages in Figure 3-4. It is evident from the comparison that the average transport rates measured at the two analog sites are similar to those shown for undisturbed grassland and woodland (2.0 and 1.4 g/m^2/d [4.1×10^{-4} and 2.9×10^{-4} lb/ft^2/d], respectively).

3.1.4   Aerosol Characterization

Airborne particle concentrations decrease as the diameter of the particles increase (Figure 3-5). The data suggest that most airborne particles in the sampling area are less than 10 µm (3.9×10^4 in.) and thus, are respirable. Based on considerations of settling velocities, the smallest particles (i.e., <1 µm [3.9×10^{-5} in.]) are expected to originate in distant areas. Locally generated aerosols are expected to fall in the >5 µm (2.0×10^{-4} in.) range, although particles of this size may have also originated outside of the sampling area.
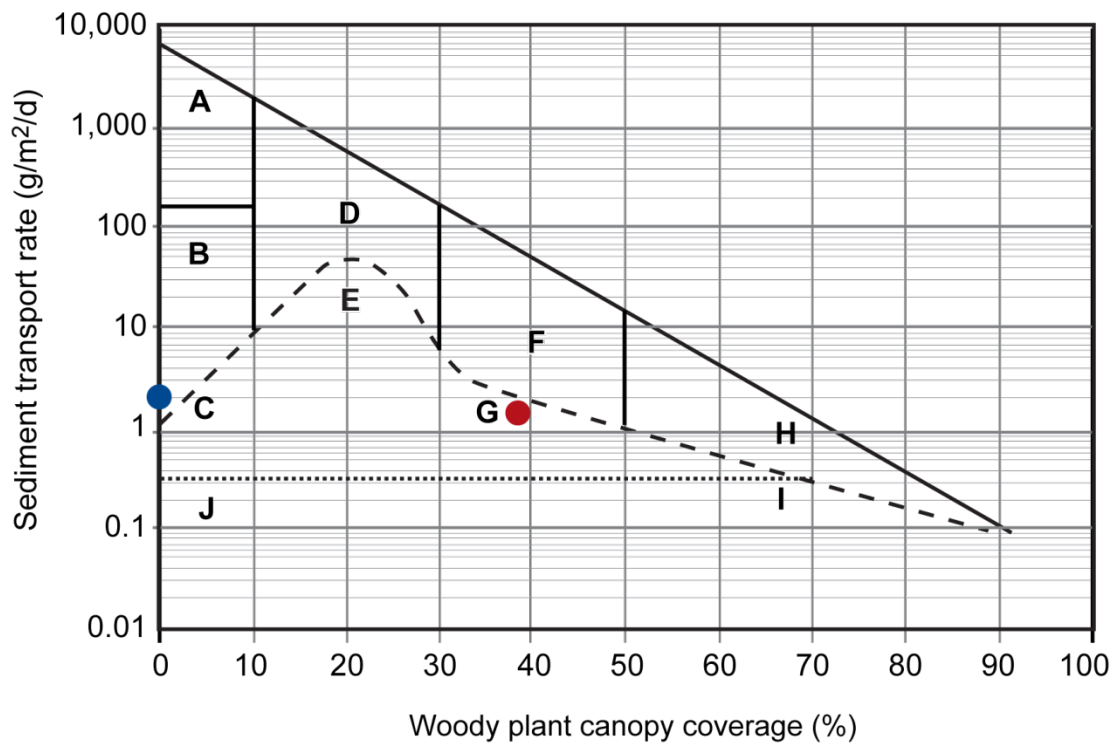
Particle concentrations were measured intermittently at MDA J and averaged over periods of time ranging from 5 minutes to an hour. Concentration profiles collected at 5-minute intervals showed the most variation with time; these concentrations are shown in Figure 3-6 (on some occasions the concentrations for the 0.3- to 0.5-µm size particles are off the scale and thus appear to be missing). The concentrations were greatest for the smallest particles (<1 µm [3.9×10^{-5} in.] diameter); concentrations spiked on numerous occasions, most notably for large particles, which suggests local suspension. The easily discernible fluctuations in the measurements may indicate that the Climet measurements are sensitive indicators of threshold phenomenon.
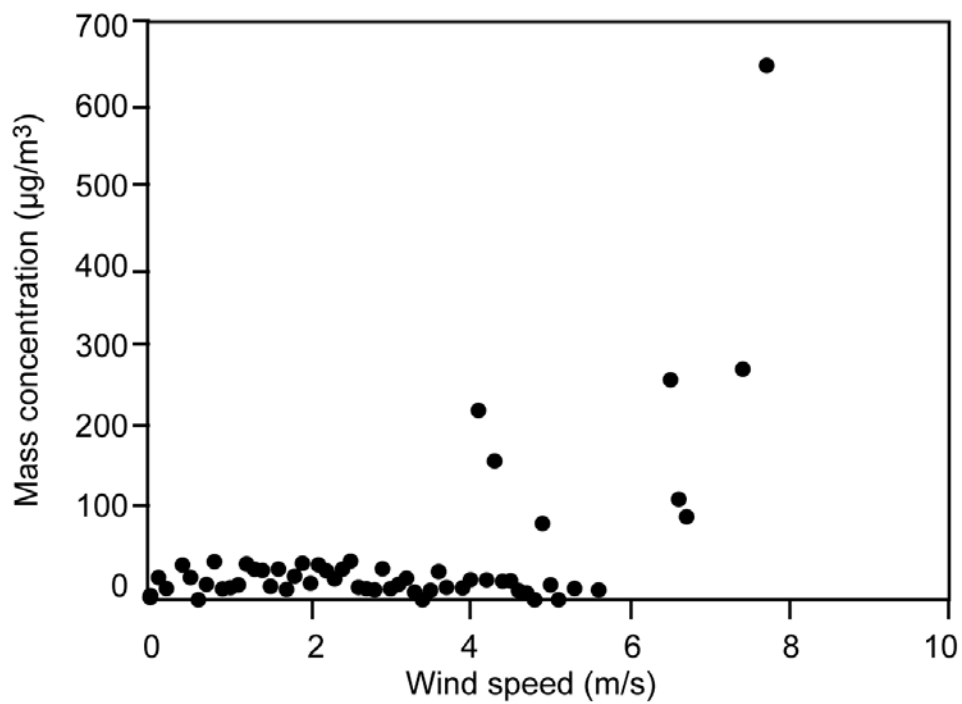
Figure 3-2
**Mass Concentration Measured at TA-6 as a Function of Wind Speed**
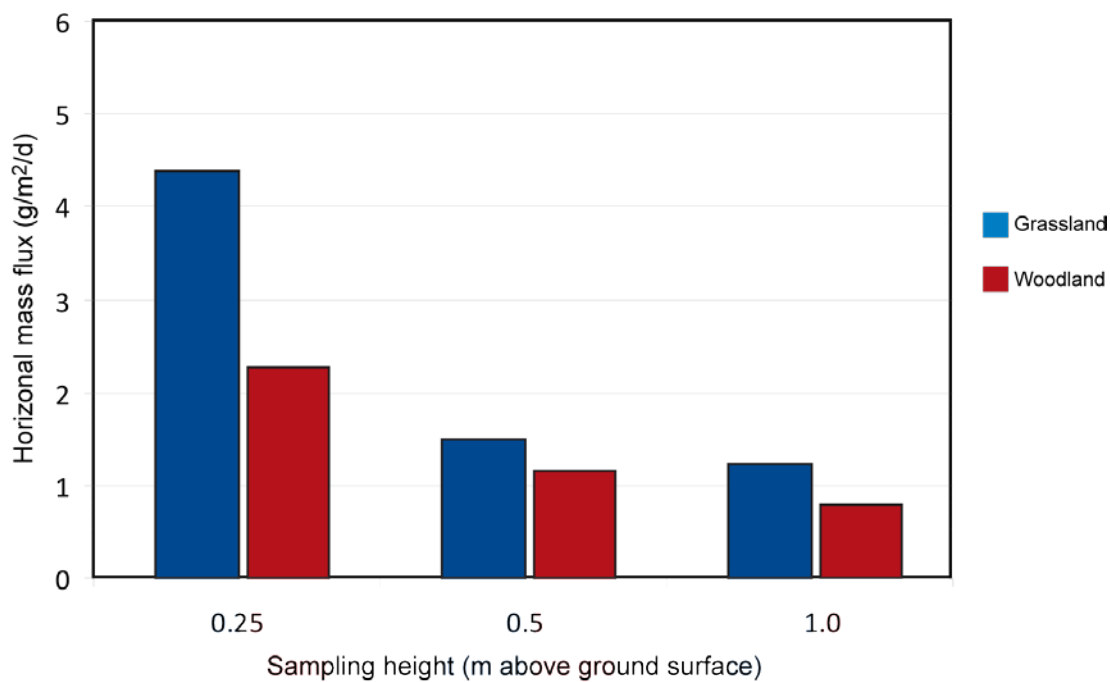
Figure 3-3
Horizontal Mass Flux, by Sampling Height, for the
Grassland and Woodland Analog Sites

Category	Description	Nominal sediment transport rate (g/m²/d)
A	Bare - no woody canopy cover	2000
B	Grassland - moderately disturbed	60
C	Grassland - undisturbed	2
D	Shrubland - disturbed	120
E	Shrubland - undisturbed	20
F	Woodland - disturbed	8
G	Woodland - undisturbed	1.4
H	Forest - disturbed	1.2
I	Forest - undisturbed	0.4
J	High ground cover	0.2
🔵	Average flux measured at grassland site	
🔴	Average flux measured at woodland site	

Figure 3-4
Comparison of Sediment Transport Rates Measured at Area J and Mesita del Buey to Rates Used in VMTran Model
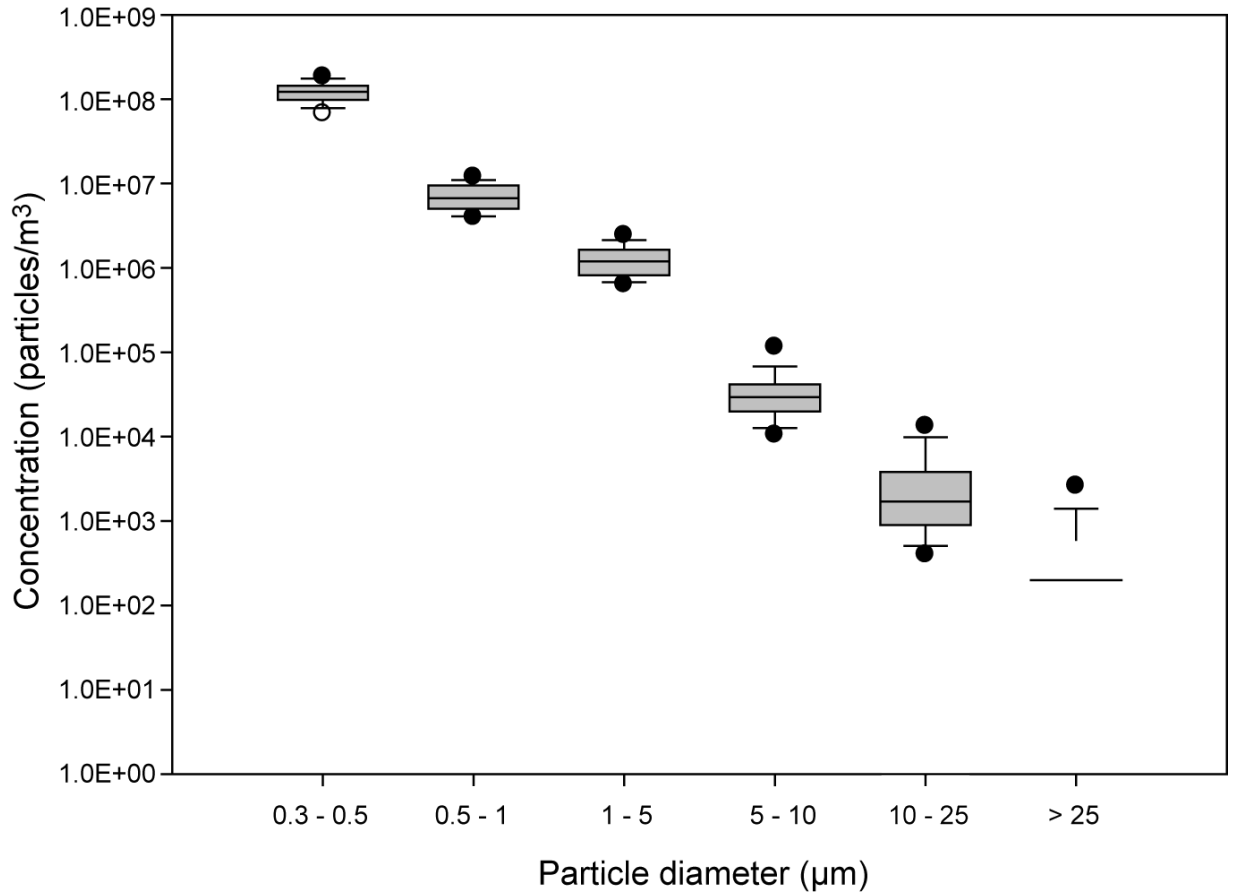
Figure 3-5
Particle Concentrations as a Function of Particle Diameter
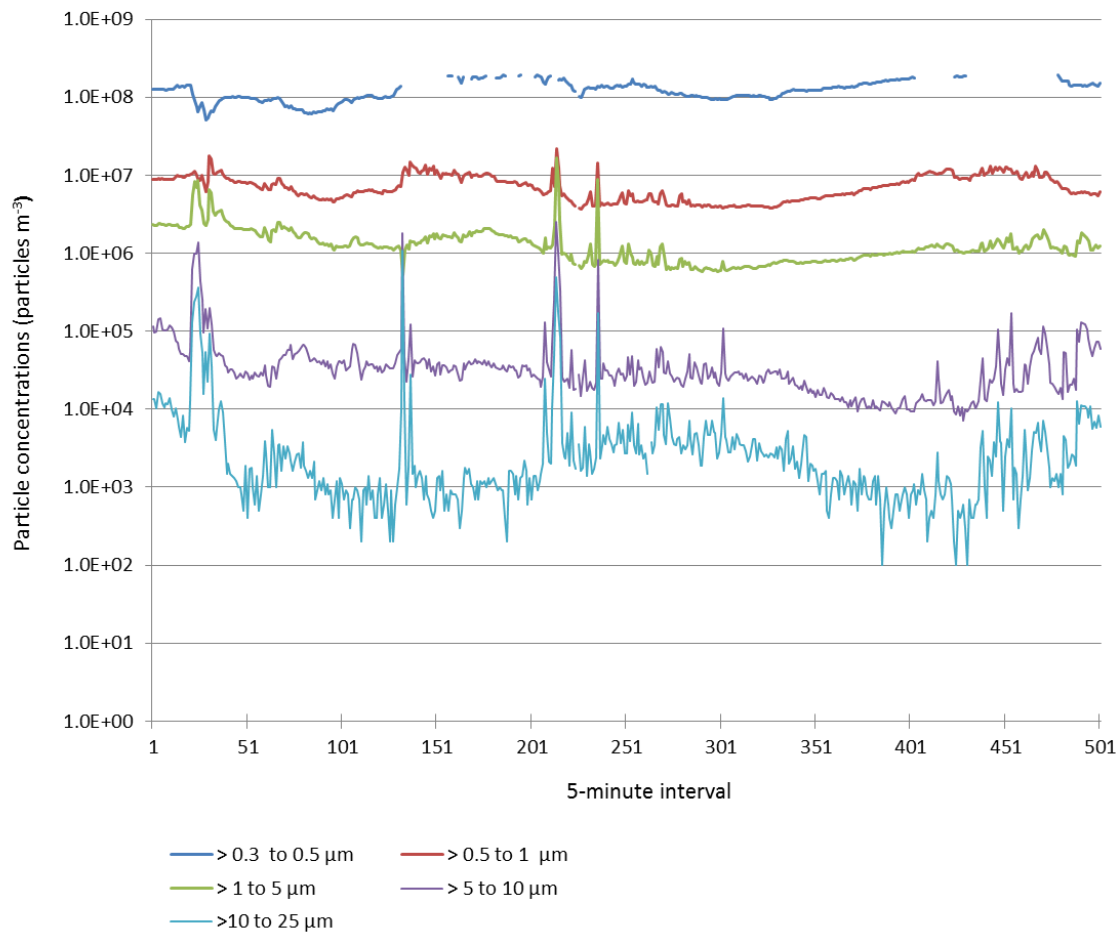
Figure 3-6
Time Profile of Aerosol Concentrations Averaged over 5-Minute Intervals
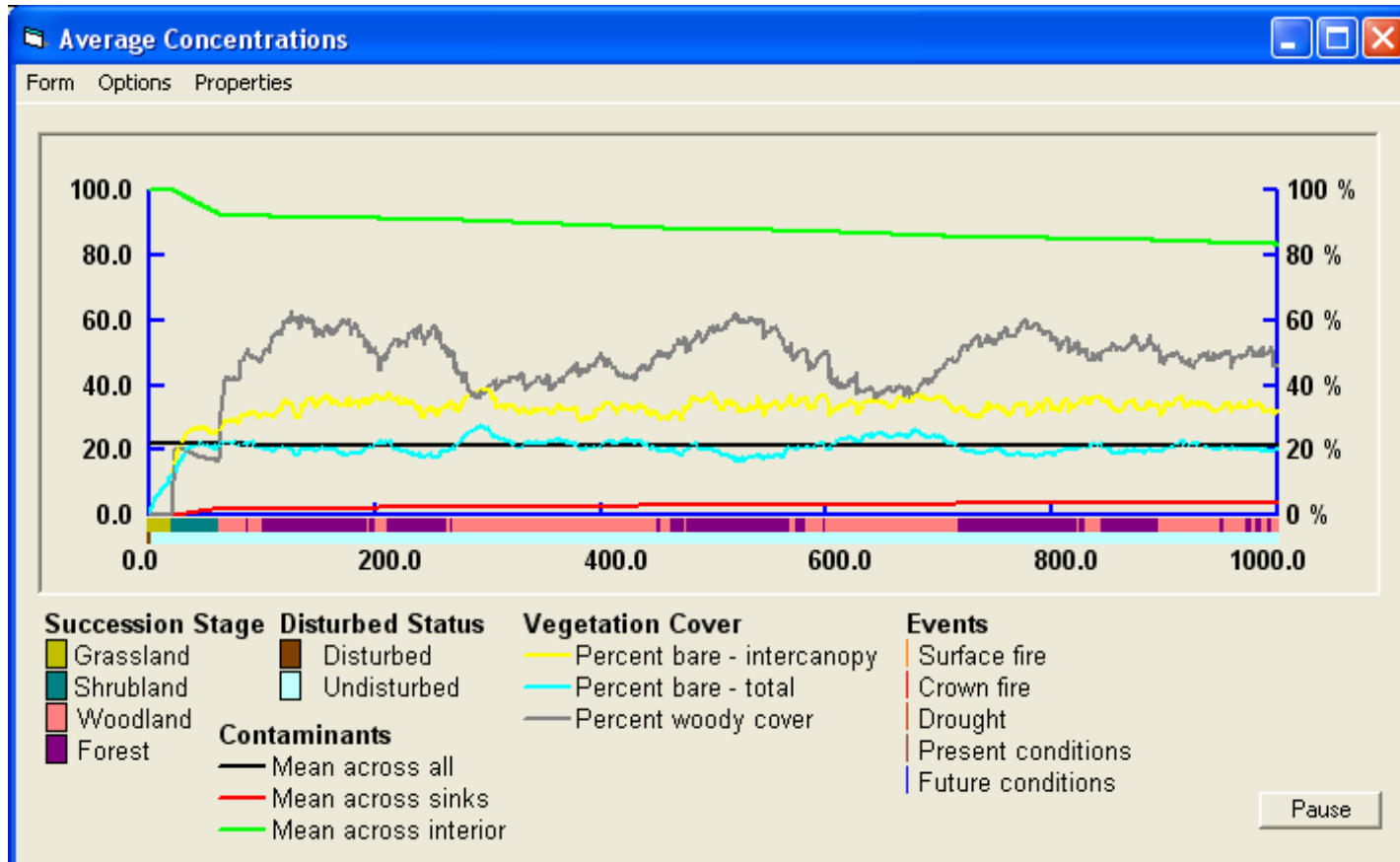
3.2 Model Simulation Results

The results of the VMTran simulations are shown in a series of screen shots taken from the program (Figures 3-7 through 3-12). The results for the succession-only simulation are shown in Figure 3-7; this simulation assumes current climatic conditions and no disturbances during the 1,000-year simulation period. The left-hand y-axis represents relative soil contaminant concentrations, while the right-hand y-axis reflects the condition of the vegetation cover. The x-axis shows the passage of time; in addition, indicators along this axis specify if the modeled system is in a disturbed or undisturbed state and display the successional stage of the site. The results for this simulation indicate a relatively rapid loss of contaminated sediment over the first 100 years; contaminant concentrations in the interior cells (i.e., the initial zone of contamination) decrease by about 15 percent, while concentrations in the off-site or sink cells, which are located on the periphery of the site, rise. These changes reflect the transport of contaminated sediment offsite. Rates of sediment transport (and contaminant loss) slow as grassland transitions to shrubland and piñon-juniper woodland. The site exists as woodland over the last 900 years of the simulation; the woodland and forest designations shown in the figure represent piñon-juniper woodland with moderate and high canopy cover, respectively. Contaminant concentrations decline slowly over this period, reflecting low rates of sediment loss; approximately 80 percent of the contamination remains on site after 1,000 years.

More complex patterns of sediment transport are observed when the effects of disturbances are taken into account. Figures 3-8 through 3-11 provide VMTran model projections for the disturbed case under current climatic conditions. Separate results are provided for the different types of disturbance and for all disturbances combined. The results for surface fire (Figure 3-8) tend to show the greatest impact on the fraction of the site surface that is bare soil; rates of increase of woody cover are slowed and occasionally reversed by fire. Rates of sediment (and contaminant) loss tend to be stable when woody cover is high and prone to increase when woody cover drops. This is most evident at about year 850, at which time woody cover drops significantly in response to successive surface fires.

Crown fires are less frequent but tend to have greater impacts on woody cover and, therefore, sediment transport (Figure 3-9). The fire early in the simulation period has little impact because woody cover has not yet been established. Later disturbances remove all woody cover and rates of sediment transport increase in its absence; a 20 percent reduction in on-site contamination occurs over a period of about 200 years. Rates of sediment and contaminant transport are more stable late in the simulation period, after the fires have passed and woody vegetation has been re-established.

Drought has its greatest impact on the growth of grasses and forbs (Figure 3-10). The amount of woody cover present oscillates during the simulation period but remains relatively constant. As a result, large variations in sediment transport are absent. When the effects of drought are combined with those seen for surface and crown fires, a complex pattern of sediment transport is seen (Figure 3-11).

Figure 3-7
Simulation Results for Changes in Successional Stage in the
Absence of Environmental Disturbances
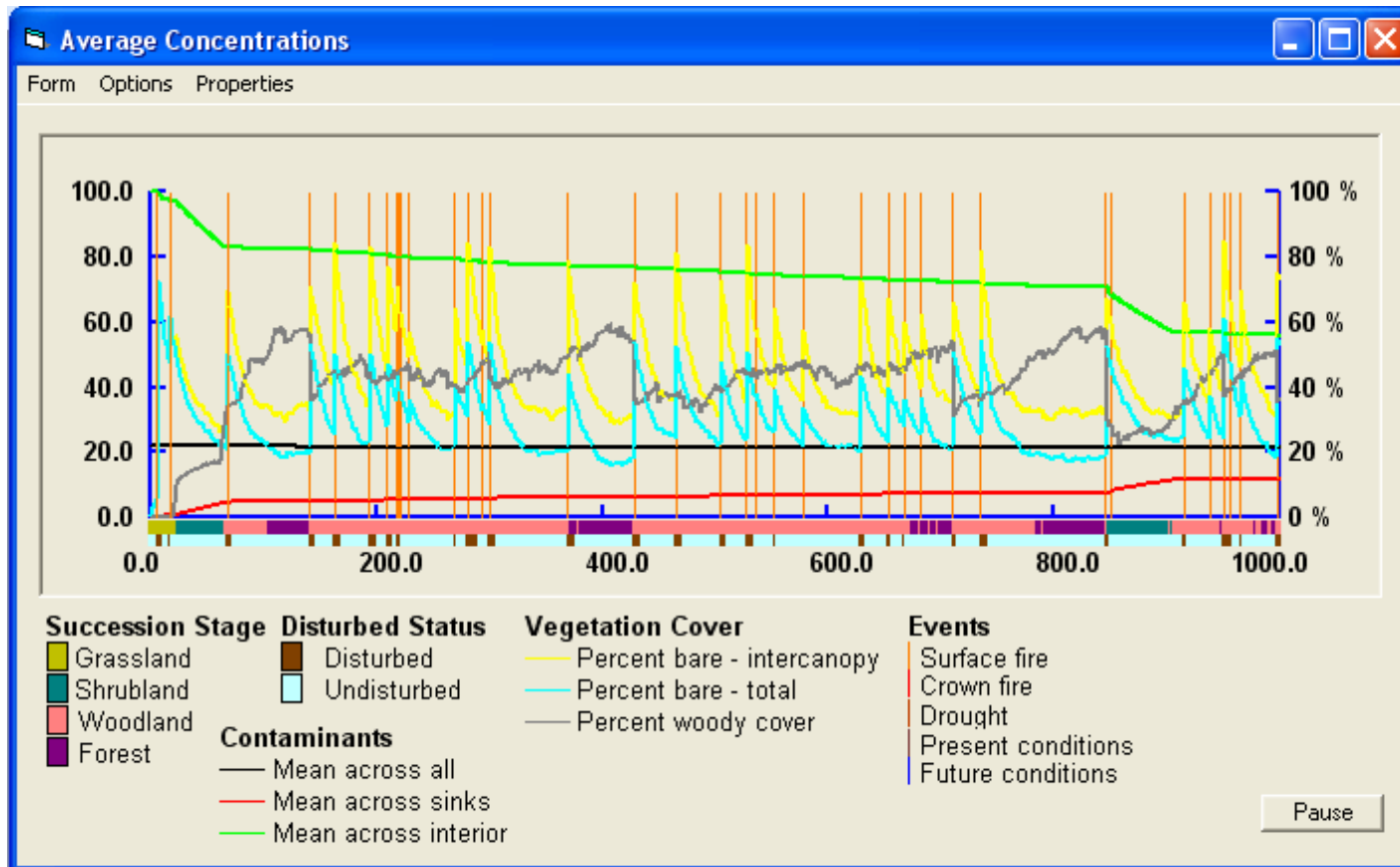
Figure 3-8
Simulation Results for Changes in Successional Stage Accompanied by Surface
Fire Disturbances under Current Climatic Conditions
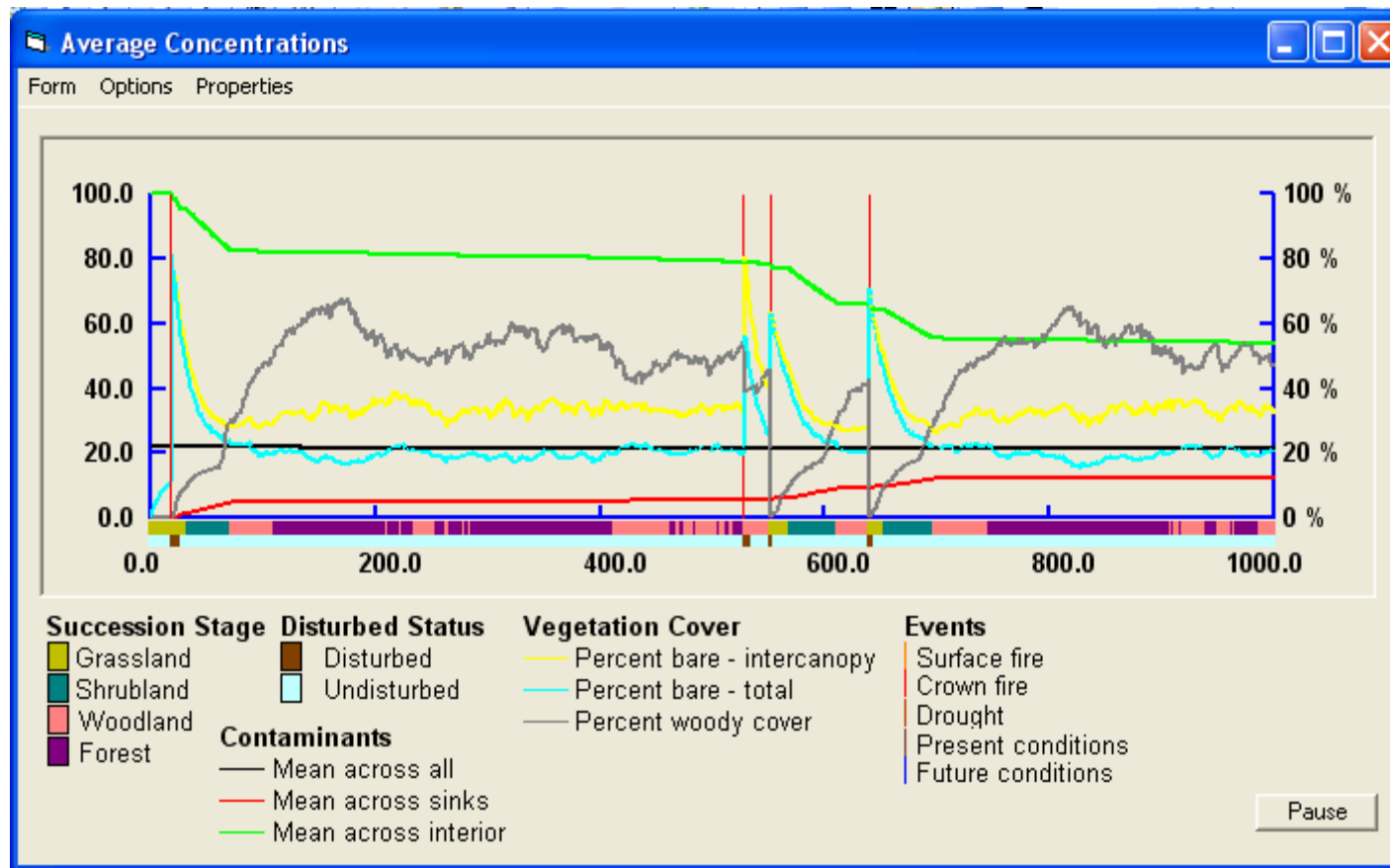
Figure 3-9
Simulation Results for Changes in Successional Stage Accompanied by Crown
Fire Disturbances under Current Climatic Conditions
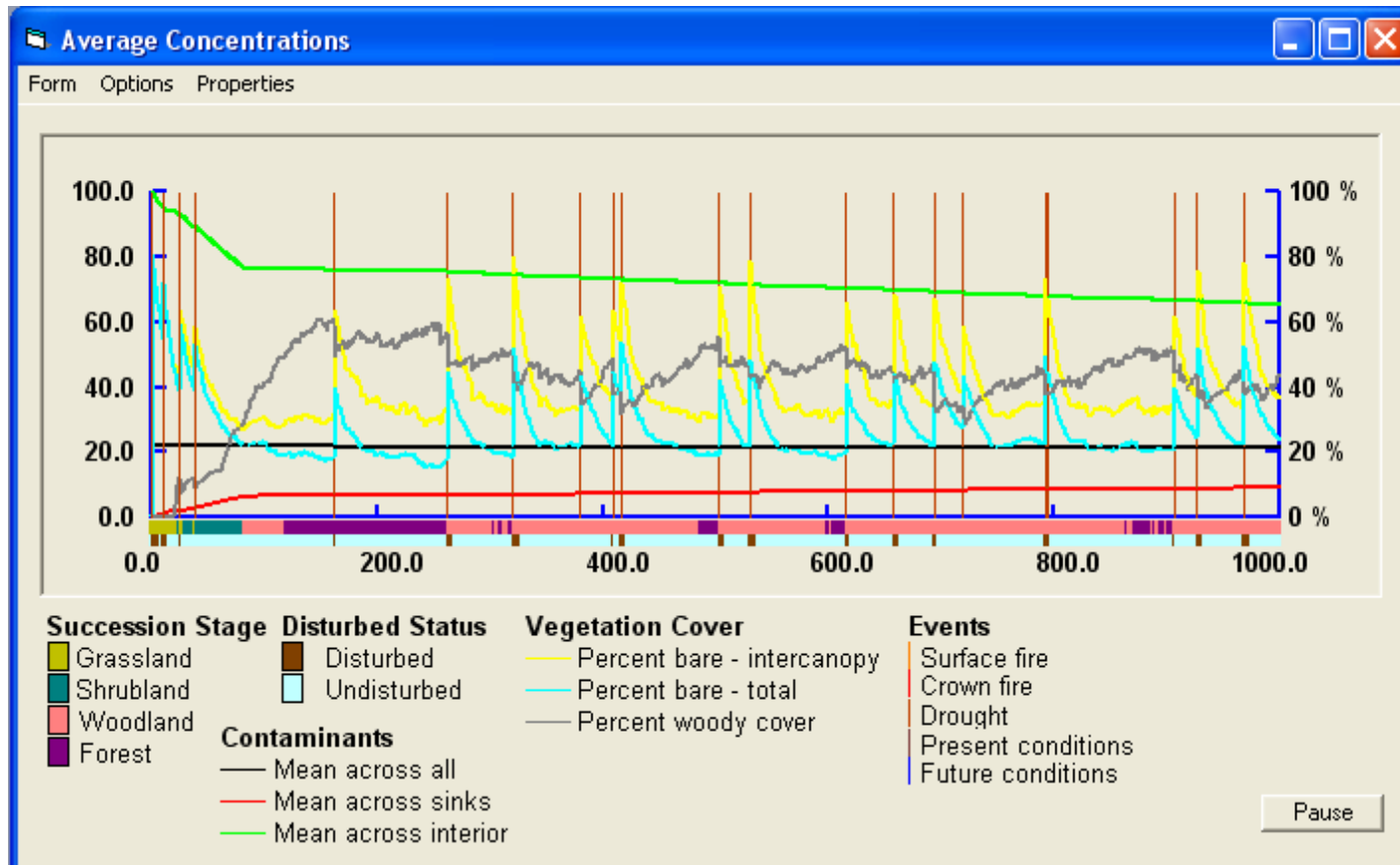
Figure 3-10
Simulation Results for Changes in Successional Stage Accompanied by
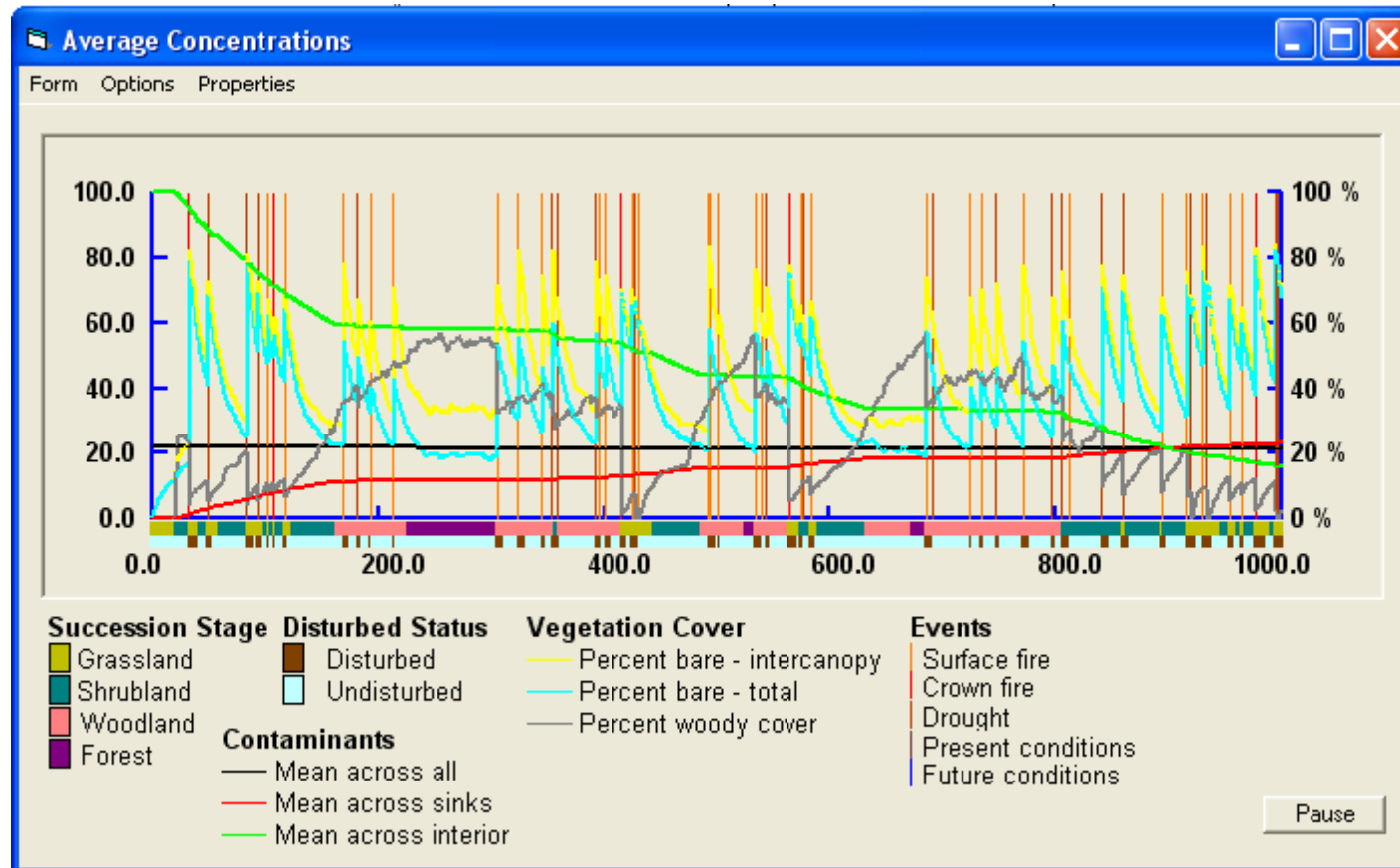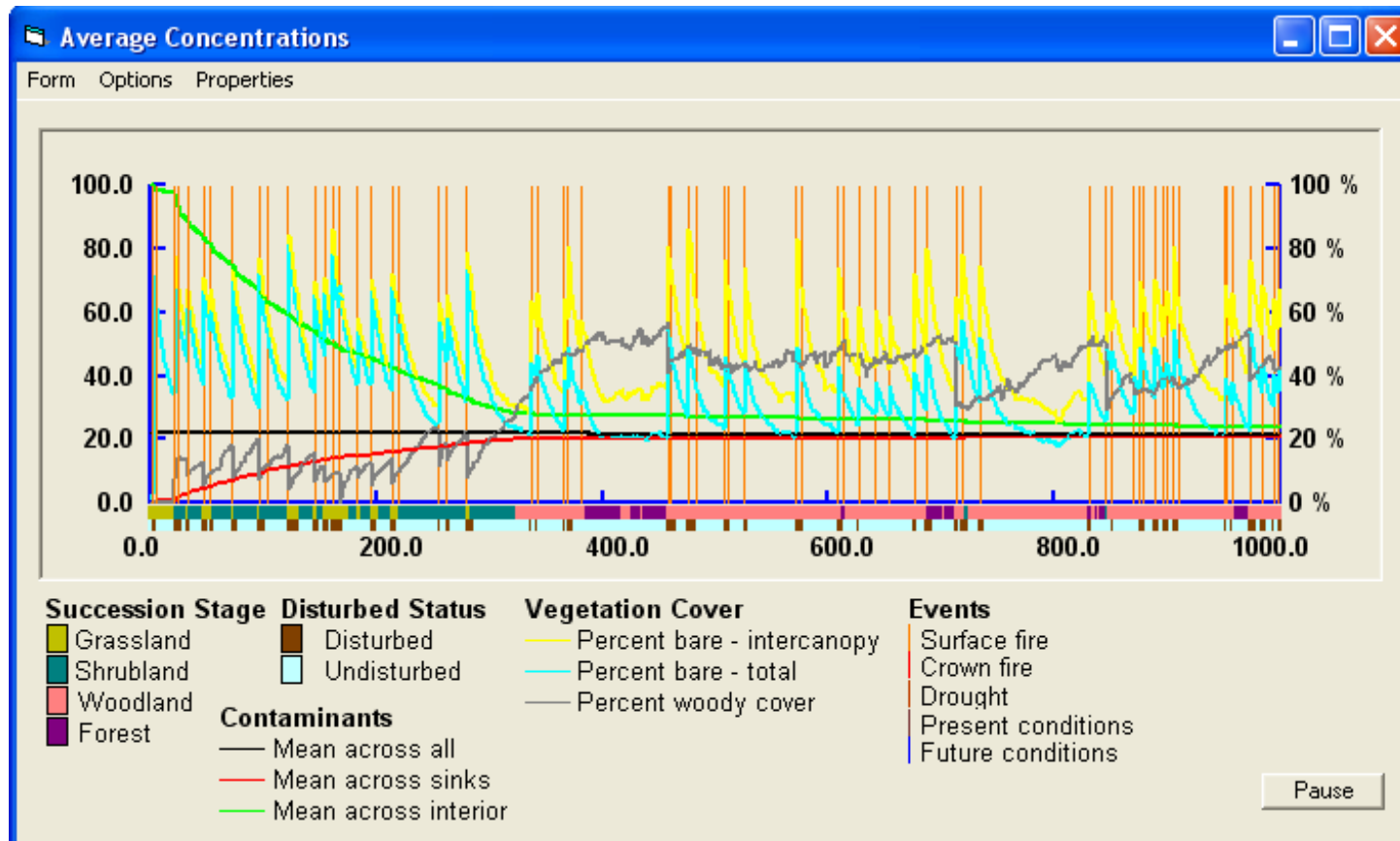**Drought (50 yr) under Current Climatic Conditions**

Figure 3-11
Simulation Results for Changes in Successional Stage Accompanied by
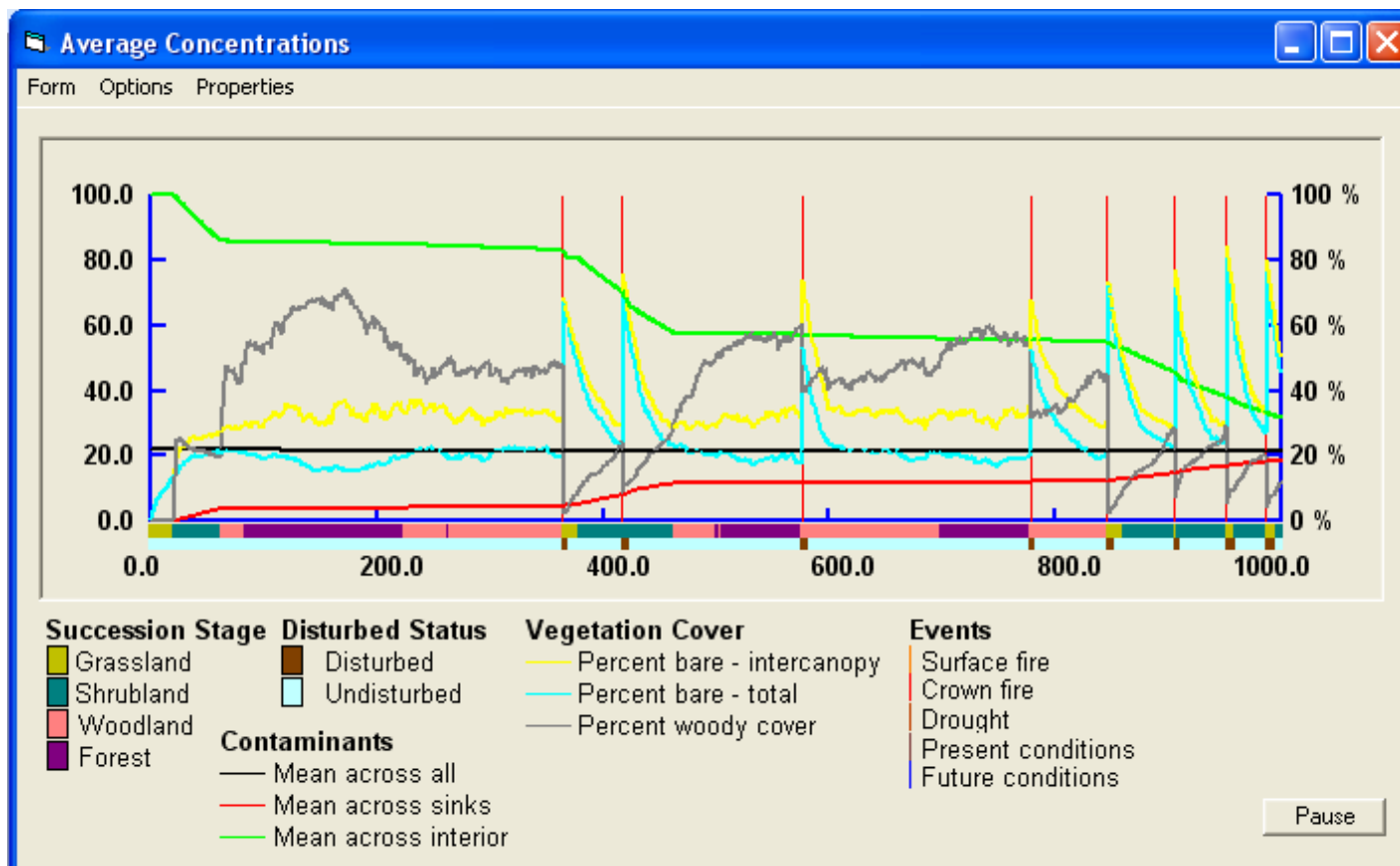**All Disturbances under Current Climatic Conditions**

The VMTran model projections for more frequent disturbances brought about by changes in the future climate are shown in Figures 3-12 through 3-15. More frequent surface fires maintain woody cover at low levels for the first 300 years of the simulation and sediment transport rates are correspondingly high (Figure 3-12); woody cover eventually becomes established and transport rates decline. Crown fires all but eradicate woody cover from the site and tend to be accompanied by large short-term increases in sediment transport rates (Figure 3-13). Because of its frequency, drought maintains woody cover at low levels for most of the 1,000-year simulation period and rates of sediment transport are high as a result (Figure 3-14). Combining all of the disturbances reveals high sediment transport rates throughout the simulation (Figure 3-15). Approximately 5 percent of the initial contamination remains on site after 1,000 years; off-site contaminant concentrations are about 25 percent of the initial on-site concentration.

The dramatic difference in the projected transfer rates of contaminated soil off site following disturbances is driven by the changing transport rate, which is a dynamic parameter in the VMTran model. Figure 3-16 shows how the transport rate varies in response to changes in vegetative cover and disturbance. In Figure 3-16a, sediment transport rate is shown as a function of time in the absence of disturbance; relatively high transport rates are observed when the site exists as grassland or shrubland, but these decrease over time as woody vegetation becomes established. When the site is disturbed, higher rates of transport are sustained over longer periods of time because the site exists as grassland or shrubland for a larger portion of the simulation period (Figure 3-16b).

The simulation results show the importance of including vegetation dynamics in long-term risk assessment, but the specific results of the simulations should be viewed with caution. Although the data used in the modeling are pertinent to Area G, the long-term behavior of the disposal facility will likely differ from the projections shown here. For simplicity, the simulations provided in this report assume a finite source of contamination uniformly dispersed across the surface. In fact, contaminant concentrations at Area G will vary across the site, with depth, and over time as plants and animals intrude into the disposal units and deposit contamination on the soil surface. Consideration of these dynamics will have a significant impact on the rates at which radionuclides are redistributed across the site and transported into the canyons bordering the disposal facility. Implementing the concepts used to develop VMTran within the full modeling framework that was used to conduct the Area G performance assessment and composite analysis modeling will be necessary to fully predict the effects of wind erosion on the long-term performance of the facility. The work presented here and the development of VMTran provide the insight and tools needed to address this facet of contaminant transport.

Figure 3-12
Simulation Results for Changes in Successional Stage Accompanied by
Surface Fire Disturbances under Future Climatic Conditions

Figure 3-13
Simulation Results for Changes in Successional Stage Accompanied by
Crown Fire Disturbances under Future Climatic Conditions
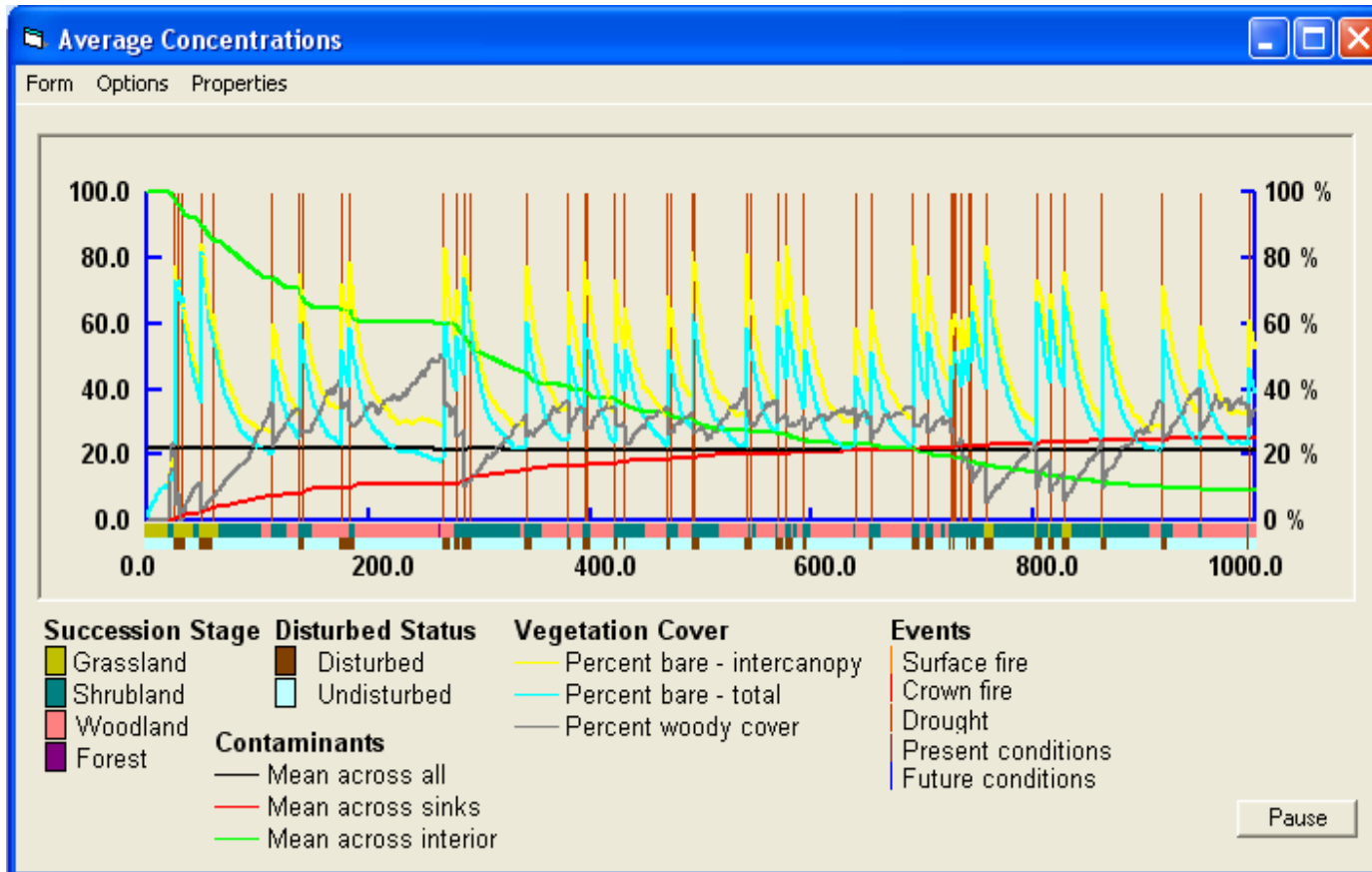
Figure 3-14
Simulation Results for Changes in Successional Stage Accompanied by
Drought under Future Climatic Conditions
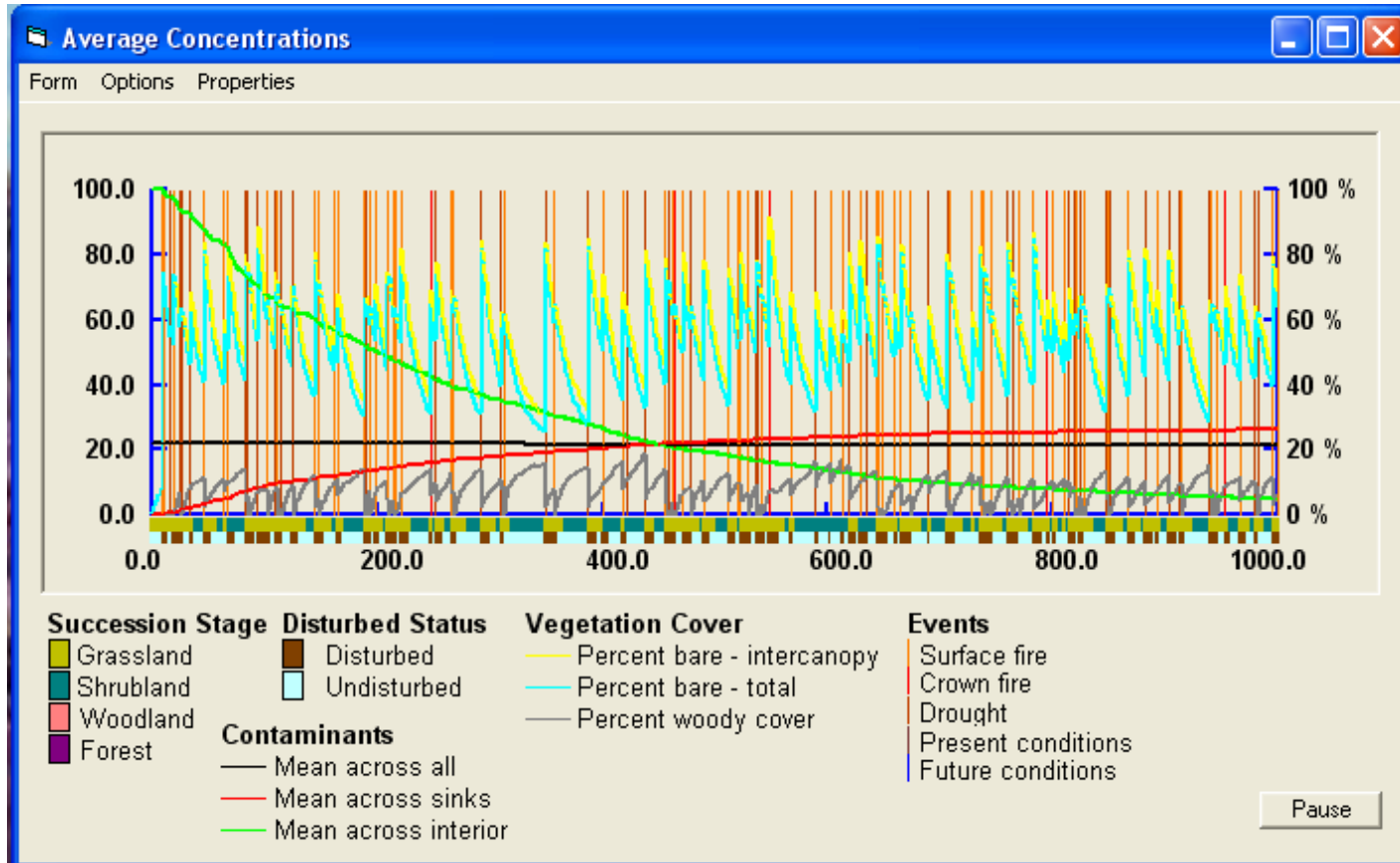
Figure 3-15
Simulation Results for Changes in Successional Stage Accompanied by
All Disturbances under Future Climatic Conditions

a. Without environmental disturbances
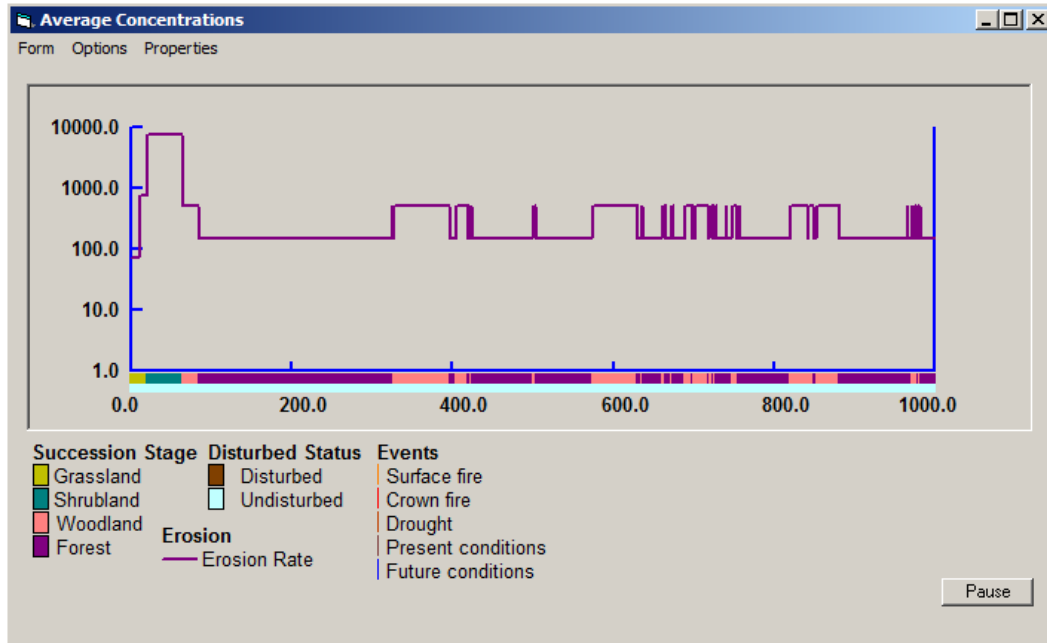
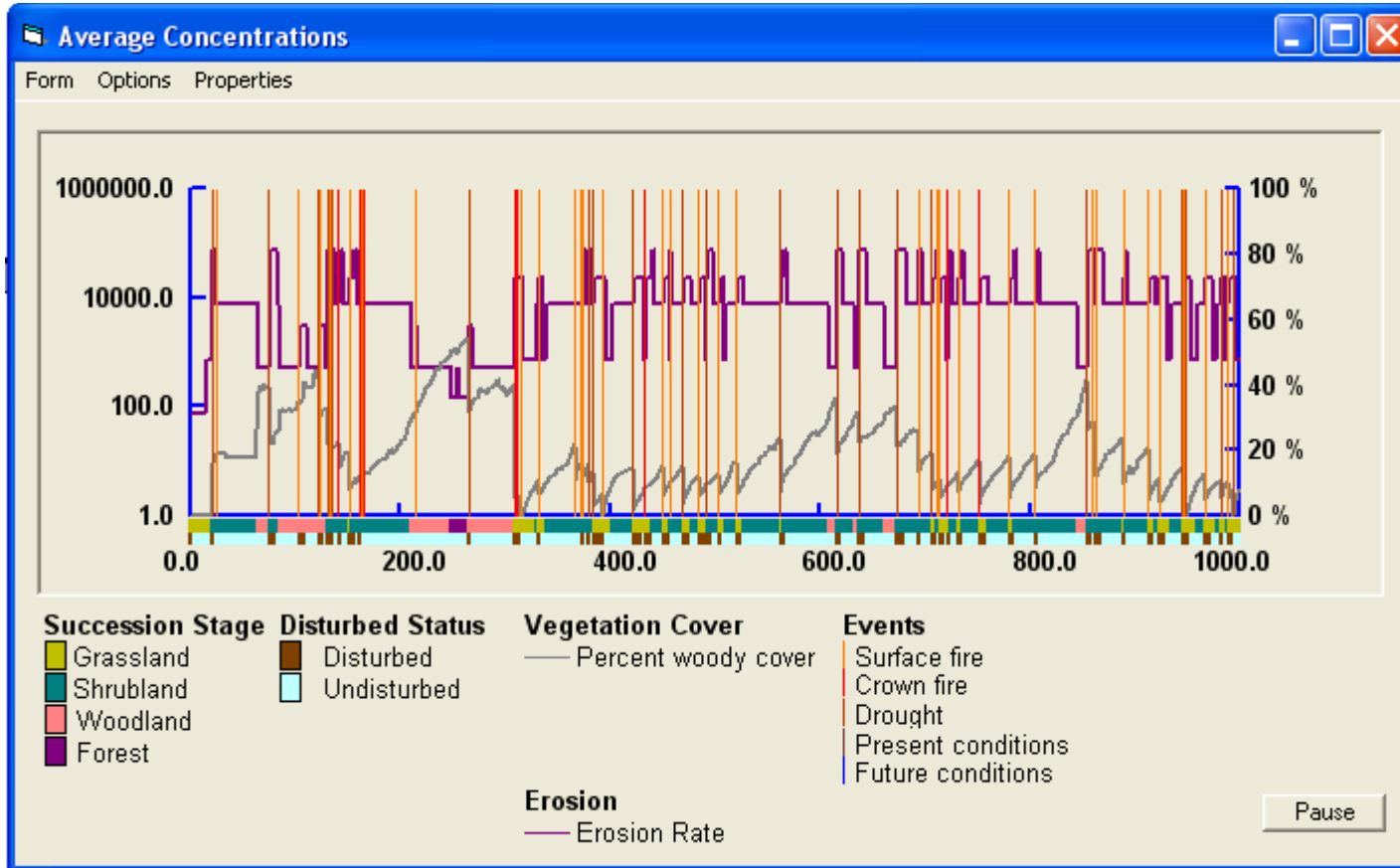b. With environmental disturbances

Figure 3-16
Sediment Flux Rates (g/m²/yr) over 1000-year Simulation Period

Figure 3-17
Sediment Transport Rates Projected for Successional Stage
Transitions and Environmental Disturbance Regimes

4.0   Discussion

The results of this investigation highlight the importance of vegetation and the impacts that disturbances may have on rates of aeolian sediment transport at dryland sites such as Area G. The sample simulations indicate that rates of sediment transport are moderated by the establishment of woody vegetation (shrubs and trees) at the site and tend to be greatest when disturbances impacted these growth forms. Crown fires cause the greatest impact because, unlike surface fire and drought, they lead to the complete removal of woody vegetation. Although generally associated with lesser impacts, surface fires and drought could prove equally as, or more, disruptive than crown fire if they occur frequently. Drought-induced plant mortality can also have a significant impact because it often kills *P. edulis,* one of the two co-dominant overstory species in the area (Breshears et al., 2005a; Gitlin et al., 2006; McDowell et al., 2008). Surface fires alter the understory, but not the amount of woody plant canopy cover; thus, the effects are less dramatic than with crown fires or drought-induced plant mortality.

As modeled here, future climatic changes are assumed to double the frequency of environmental disturbance at the disposal site. The occurrence of more frequent surface fires shortly after closure will delay the transition of Area G to woodland. Once woodland is established, however, the general impact of surface fire on the plant community is the same, despite the projected increase in frequency. An increase in the frequency of crown fires will affect the woodland regime negatively, perhaps causing it to revert to earlier successional stages; frequent droughts will also limit the development of woodlands characterized by high canopy cover. For all three types of disturbance, higher modeled frequencies increase the rates of sediment transport. The actual impacts of climatic change on rates of sediment transport will, of course, depend on how that change impacts disturbance frequency; the assumption made here (that frequencies double) may be conservative (Adams et al., 2009).

The VMTran model is based on numerous simplifying assumptions that should be considered in conjunction with the projections of sediment transport. As stated earlier, the rates of horizontal aeolian transport are based on long-term (months to years) data that have recently become available for a diverse set of dryland sites. This dataset, however, has its limitations and needs to be further developed to improve the model predictions.

Vegetation successional change was simulated with a simple Markov-like model that assumed a given probability of transition from one vegetated state to another. This is approach is a highly abstracted representation of the complex interactions that control succession. Nevertheless, the overall gross structural changes in vegetation that are projected are thought to be of sufficient detail to provide the parameters required to estimate sediment transport fluxes through time. More dynamic vegetation models could be applied (e.g., Samuels and Betancourt, 1982; Neilson,

1995; Lenihan et al., 2008), although there are trade-offs in data needs and levels of uncertainty between simple and complex models that might preclude or negate the value of using more detailed models (Peters et al., 2004).

Model results are sensitive to the timing of the disturbances; longer intervals between disturbances allow woody plants to become dominant thereby slowing sediment transport rates. As a result, the accuracy of modeling disturbance frequency is an important aspect of the modeling effort. A relatively simple approach to implementing disturbances was used in VMTran. Disturbances were assumed to occur randomly, based on average return frequencies (Romme et al., 2009), but no correlation was assumed to exist among the types of disturbance. In fact, disturbances may be correlated, as witnessed by the fact that droughts and crown fires often occur together. The VMTran model also does not consider how the disturbance type or frequency is affected by the current vegetation state. Factors such as these will influence projections of disturbance frequency and, therefore, the estimated sediment transport rates.

Despite these shortcomings, the VMTran model is flexible enough to add additional complexity and can be the basis for more mechanistic or detailed approaches if needed in the future. More generally, this approach represents a fundamental next step toward incorporating major changes in vegetation due to succession, disturbance, and future climate into predictions of aeolian sediment transport.

5.0   References

Adams, H.D., Guardiola-Claramonte, M., Barron-Gafford, G.A., Villegas, J.C., Breshears, D.D., Zou, C.B., Troch, P.A., Huxman, T.E., 2009. Temperature sensitivity of drought-induced tree mortality portends increased regional die-off under global-change-type drought. *Proc. Nat. Acad. Sci. USA,* Vol. 106, pp. 7063–7066.

Allen, C.D., 2007. Interactions across spatial scales among forest dieback, fire, and erosion in northern New Mexico landscapes. *Ecosystems*, Vol. 10, pp. 797–808.

Baas, A.C.W., 2002. Chaos, fractals and self-organization in coastal geomorphology: simulating dune landscapes in vegetated environments. *Geomorphology*, Vol. 48, p. 309–328.

Baas, A.C.W., Nield, J.M., 2007. Modelling vegetated dune landscapes. *Geophys. Res. Lett*. Vol. 34, L06405.

Baas, A.C.W., Nield, J.M., 2010. Ecogeomorphic state variables and phase-space construction for quantifying the evolution of vegetated aeolian landscapes. *Earth Surf. Proc. Land*., Vol. 35, 717–731.

Baldocchi, D., 1997. Flux footprints within and over forest canopies. *Boundary Layer Meteorol*., Vol. 8, pp. 273–292.

Bergametti, G., Gillette, D.A., 2010. Aeolian sediment fluxes measured over various plant/soil complexes in the Chihuahuan desert*. J. Geophy. Res*., Vol. 115, F03044. doi:10.1029/2009JF001543.

Breshears, D.D., Cobb, N.S., Rich, P.M., Price, K.P., Allen, C.D., Balice, R.G., Romme, W.H., Kastens, J.H., Floyd, M.L., Belnap, J., Anderson, J.J., Myers, O.B., Meyer, C.W., 2005a. Regional vegetation die-off in response to global-change-type drought, *Proc. Nat. Acad. Sci. USA,* Vol. 102, pp. 15144–15148.

Breshears, D.D., Nyhan, J.W., Davenport, D.W., 2005b. Ecohydrology monitoring and excavation of semiarid landfill covers a decade after installation. *Vadose Zone J*., Vol. 4, p. 500–504.

Breshears, D.D., Whicker, J.J., Zou, C.B., Field, J.P., Allen, C.D., 2009. A conceptual framework for dryland aeolian sediment transport along the grassland–forest continuum: effects of woody plant canopy cover and disturbance. *Geomorphology*, Vol. 105, pp. 28–38.

Chadwick, O.A., Derry, L.A., Vitousek, P.M., Huebert, B.J., Hedin, L.O., 1999. Changing sources of nutrients during four million years of ecosystem development. Nature 397, 491-497.

DOE, 2001, *Radioactive Waste Management,* U.S. Department of Energy Order DOE O 435.1 (change 1 to document issued July, 9, 1999), August 28.

Dong, Z.B., Man, D.Q., Luo, W.Y., Qian, G.Q., Wang, J.H., Zhao, M., Liu, S.Z., Zhu, G.Q., Zhu, S.J., 2010. Horizontal aeolian sediment flux in the Minqin area, a major source of Chinese dust storms. *Geomorphology*, Vol. 116, pp. 58–66.

Díaz-Nigenda, E., Tatarko, J., Jazcilevich, A.D., García, A.R., Caetano, E., Ruíz-Suárez, L.G., 2010. A modeling study of Aeolian erosion enhanced by surface wind confluences over Mexico City. *Aeolian Res.* doi:10.1016/j.aeolia.2010.04.004.

Field, J.P., Belnap, J., Breshears, D.D., Neff, J.C., Okin, G.S., Whicker, J.J, Painter, T.H., Ravi, S., Reheis, M.C., Reynolds R.L., 2010. The ecology of dust. *Front. Ecol. Environ.*, Vol. 8, pp. 423–430. doi:10.1890/090050.

Flores-Aqueveque, V., Alfaro, S., Munoz, R., Rutllant, J.A., Caquineau, S., Le Roux, J.P., Vargas, G., 2010. Aeolian erosion and sand transport over the Mejillones Pampa in the coastal Atacama Desert of northern Chile. Geomorphology 120, 312-325.

Fryrear, D.W., 1986. A field dust sampler. *J. Soil Water Conserv.*, Vol. 41, pp. 117–120.

Gillette, D.A., Chen, W., 2001. Particle production and aeolian transport from a 'supply-limited' source area in the Chihuahuan Desert, New Mexico, United States. *J. Geophys. Res.* Vol. 106, pp. 5267–5278.

Gillette, D.A., Passi, R., 1988. Modeling dust emission caused by wind erosion. *J. Geophys. Res.-Atmos.*, Vol. 93, pp. 14233–14242.

Gitlin A.R., C.M. Sthultz, M.A. Bowker, S. Stumpf, K.L. Paxton, K. Kennedy, A. Munoz, J.K. Bailey, and T.G. Whitham. 2006. Mortality gradients within and among dominant plant populations as barometers of ecosystem change during extreme drought. *Conservation Biology*, Vol. 20, pp. 1477–1486.

Glenn-Lewin, D.C., van der Maarel, E., 1992. Patterns and processes of vegetation dynamics. *Plant Succession, Theory and Prediction*, (eds D.C. Glenn- Lewin, R.K. Peet, T.T. Veblen), Chapman & Hall, London., pp. 11–59.

Herrick, J.E., Van Zee, J.W., Havstad, K.M., Burkett, L.M., Whitford, W.G., 2005. Monitoring manual for grassland, shrubland, and savannah ecosystems. Volume 1: Quick Start. Publisher: USDA-ARS Jornado Experimental Range, P.O. Box 30003, MSC 3JER, New Mexico State University, Las Cruces, NM.

Horn, H. S., 1974. The ecology of secondary succession. Annual Review of Ecology and Systematics, Vol. 5, pp. 25–37.

Huston, M., Smith, T., 1987. Plant succession – Life-history and competition. *Am. Nat.* Vol. 130, pp. 168–198.

Jickells, T.D., An, Z.S., Andersen, K.K., Baker, A.R., Bergametti, G., Brooks, N., Cao, J.J., Boyd, P.W., Duce, R.A., Hunter, K.A., Kawahata, H., Kubilay, N., laRoche, J., Liss, P.S., Mahowald, N., Prospero, J.M., Ridgwell, A.J., Tegen, I., Torres, R., 2005. Global iron

connections between desert dust, ocean biogeochemistry, and climate. *Science*, Vol. 308, pp. 67–71.

Kim, D., Yu, K.B., 2009. A conceptual model of coastal dune ecology synthesizing spatial gradients of vegetation, soil, and geomorphology. *Plant Ecol.* Vol. 202, pp. 135–148.

LANL, 2008, *Performance Assessment and Composite Analysis for Los Alamos National Laboratory Technical Area 54, Area G, Revision 4,* Los Alamos National Laboratory Report LA-UR-08—6764, October.

Lee, J.A., 1991. The role of desert shrub size and spacing on wind-profile parameters. *Phys. Geog*., Vol. 12, pp. 72–89.

Lenihan, J.M., Bachelet, D., Neilson, R.P., Drapek, R., 2008. Simulated response of conterminous United States ecosystems to climate change at different levels of fire suppression, CO_2 emission rate, and growth response to CO_2. *Global Planet. Change*, Vol. 64,pp. 16–25.

Li, J., Okin, G.S., Hartman, L.J., Epstein, H.E., 2007. Quantitative assessment of wind erosion and soil nutrient loss in desert grasslands of southern New Mexico, USA. *Biogeochemistry*, Vol. 85, pp. 317–332.

Martens, S.N., Breshears, D.D., Meyer, C.W., Barnes, F.J., 1997. Scales of above-ground and below-ground competition in a semi-arid woodland detected from spatial pattern. *J. Veg. Sci*., Vol. 8, pp. 655–664.

McDowell, N., Pockman, W.T., Allen, C.D., Breshears, D.D., Cobb, N., Kolb, T., Plaut, J., Sperry, J., West, A., Williams, D.G., 2008. Mechanisms of plant survival and mortality during drought: why do some plants survive while others succumb to drought? *New Phytol*., Vol. 178, pp. 719–739.

Neff, J.C., Ballantyne, A.P., Famer, G.L., Mahowald, N.M., Conroy, J.L., Landry, C.C., Overpeck, J.T., Painter, T.H., Lawrence, C.R., Reynolds, R.L. 2008. Increasing eolian dust deposition in the western United States linked to human activity. *Nature – Geosciences*. doi:10.1038/ngeo133.

Neilson, R.P., 1995. A model for predicting continental-scale vegetation distribution and water-balance. *Ecol. Appl*., Vol. 5, pp. 362–385.

Nield, J.M., Baas, A.C.W., 2008. Investigating parabolic and nebkha dune formation using a cellular automaton modelling approach. *Earth Surf. Proc. Land*., Vol. 33, pp. 724–740.

Okin, G.S., 2008. A new model of wind erosion in the presence of vegetation. *J Geophys. Res.–Earth Surf*., Vol. 113, F02S10.

Okin, G.S., Gillette, D.A., 2001. Distribution of vegetation in wind-dominated landscapes: Implications for wind erosion modeling and landscape processes. *J. Geophys. Res*., Vol. 106, pp. 9673–9683.

Peters, D.P.C., Herrick, J.E., Urban, D.L., Gardner, R.H., Breshears, D.D., 2004. Strategies for ecological extrapolation. *Oikos,* Vol. 106, pp. 627–636.

Pickett, S.T.A., Collins, S.L., Armesto, J.J., 1987. Models, mechanisms and pathways of succession. *Bot. Rev.*, Vol. 53, pp. 335–371.

Pye, K., 1987. Aeolian dust and dust deposits. Academic Press, Boca Raton, Florida.

Rodgers, J.C., P.T. Wasiolek, J.J. Whicker, C. Eberhart, K. Saxton, and D. Chandler, 2000, Performance Evaluation of LANL Environmental Radiological Air Monitoring Inlets at High Wind Velocities Associated with Resuspension, Los Alamos National Laboratory Report LA-UR-00-3091.

Romme, W.H., Allen, C.D., Bailey, J.D., Baker, W.L., Bestelmeyer, B.T., Brown, P.M., Eisenhart, K.S., Floyd, M.L., Huffman, D.W., Jacobs, B.F., Miller, R.F., Muldavin, E.H., Swetnam, T.W., Tausch, R.J., Weisberg, P.J., 2009. Historical and modern disturbance regimes, stand structures, and landscape dynamics in pinon-juniper vegetation of the western United States. *Rangeland Ecol. Manage.*, Vol. 62, pp. 203–222.

Samuels, M.L., Betancourt, J.L., 1982. Modeling the long-term effects of fuel wood harvests on pinyon-juniper woodlands. *Environ. Manage.*, Vol. 6, pp. 505–515.

Shinn, J., Gouvieia, F., 1992. The "footprint" area influencing a high-volume air sampler. Lawrence Livermore National Laboratory report UCRL-ID-112181.

Stockton, P.H., Gillette, D.A., 1990. Field measurement of the sheltering effects of vegetation on erodible land surfaces, *Land Degrad. Rehabil.*, Vol. 2, pp. 77–85.

Swetnam, T.W., Betancourt J.L., 1998. Mesoscale disturbance and ecological response to decadal climatic variability in the American Southwest. *J. of Climate*, Vol. 11, pp. 3128–3147.

Toy, T.J., Foster, G.R., Renard, K.G., 2002. Soil Erosion: Processes, Prediction, Measurement and Control. John Wiley & Sons, New York.

Turner, M.G., Baker, W.L., Peterson, C.J., Peet, R.K., 1998. Factors influencing succession: Lessons from large, infrequent natural disturbances. *Ecosystems,* Vol. 1, pp. 511–523.

Wangler, M., Minnich, R.A., 1996. Fire and succession in pinyon-juniper woodlands of the San Bernardino Mountains. *Madrono*, Vol. 43, pp. 493–514.

Westerling, A.L., Hidalgo, H.G., Cayan, D.R., Swetnam, T.W. 2006.Warming and earlier spring increase western US forest wildfire activity. *Science*, Vol. 313, pp. 940–943.

Whicker, J.J. and D.D. Breshears, 2005, *Assessing Wind Erosion as a Contaminant Transport Mechanism for Los Alamos National Laboratory Technical Area 54, Material Disposal Area G*, Los Alamos National Laboratory Report LA-UR-05-5371, September.

Whicker, J. J., Breshears, D.D., Wasiolek, P.T, Kirchner, T.B., Tavani, R.A., Schoep, D.A., Rodgers, J.C., 2002. Temporal and spatial variation of episodic wind erosion in unburned and burned semiarid shrubland. *J. Environ Qual*., Vol. 31, pp. 599–612.

Whicker, J.J., Pinder, J.E., Breshears, D.D., 2006a. Increased wind erosion form forest wildfire: Implications for contaminant-related risks. *J. Environ. Qual*., Vol. 35, pp. 468–478.

Whicker, J.J., Pinder, J.E., Breshears, D.D., Eberhart, C.F., 2006b. From dust to dose: Effects of forest disturbance on increased inhalation exposure. *Sci. Total Environ*., Vol. 368, pp. 519–530.

Wolfe, S.A., Nickling, W.G., 1993. The protective role of sparse vegetation in wind erosion. *Prog. Phys. Geog*., Vol. 17, pp. 50–68.

Zobeck, T.M., Sterk, G., Funk, R., Rajot J.L., Stout, J.E., Van Pelt, R.S., 2003. Measurement and data analysis methods for field-scale wind erosion studies and model validation. *Earth Surf. Process. Landforms* 28:1163-1188.